Detection of vibronic bands of C_3 in a translucent cloud towards HD 169454

M. R. Schmidt,[1] J. Krełowski,[2] G. A. Galazutdinov,[3]
D. Zhao,[4] M. A. Haddad,[5] W. Ubachs,[5] H. Linnartz[4]

[1]NCAC, Toruń, Poland

[2]CfA, Nicolaus Copernicus University, Toruń

[3]Instituto de Astronomia, Universidad Catolica del Norte, Antofagasta

[4]Raymond and Beverly Sackler Laboratory for Astrophysics, Leiden Observatory

[5]Department of Physics and Astronomy, LaserLaB, VU University, Amsterdam

Zakopane, 2015

Reference

Schmidt et al. (2014) MNRAS, 441, 1134
arXiv:1403.7280

Outline

C3 spectrum from the comet Ikeya

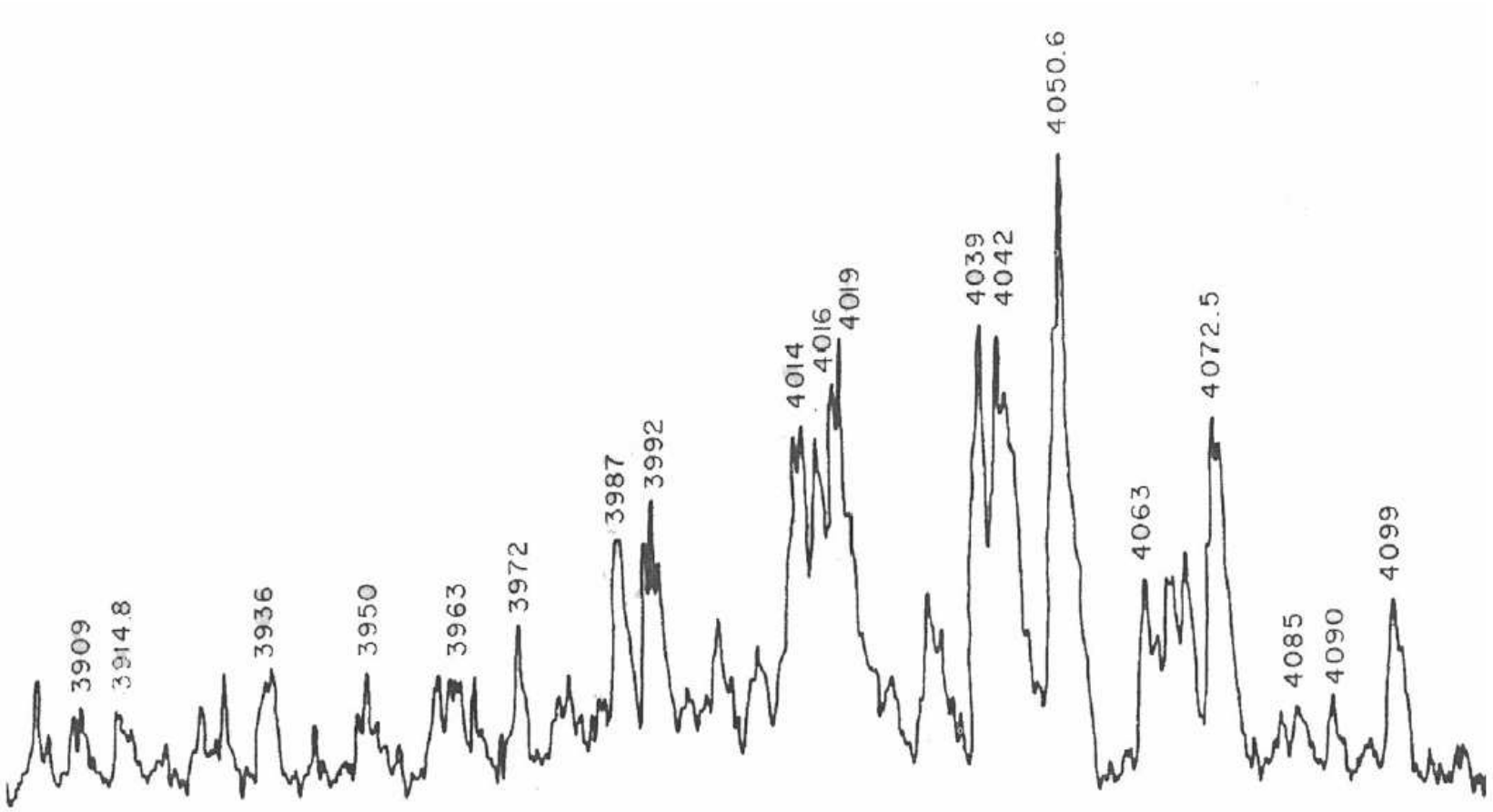

The 19th century discovery of the 4052 Å band in the spectrum of comet Tebbutt (Huggins 1881), the assignment of this blue absorption feature to the C_3 molecule made by Douglas (1951)

Vibration-rotation lines of C3 ν_3 in circumstellar shell of IRC+10216

Hinkle, Keady, & Bernath, 1988, Science, 241, 1319

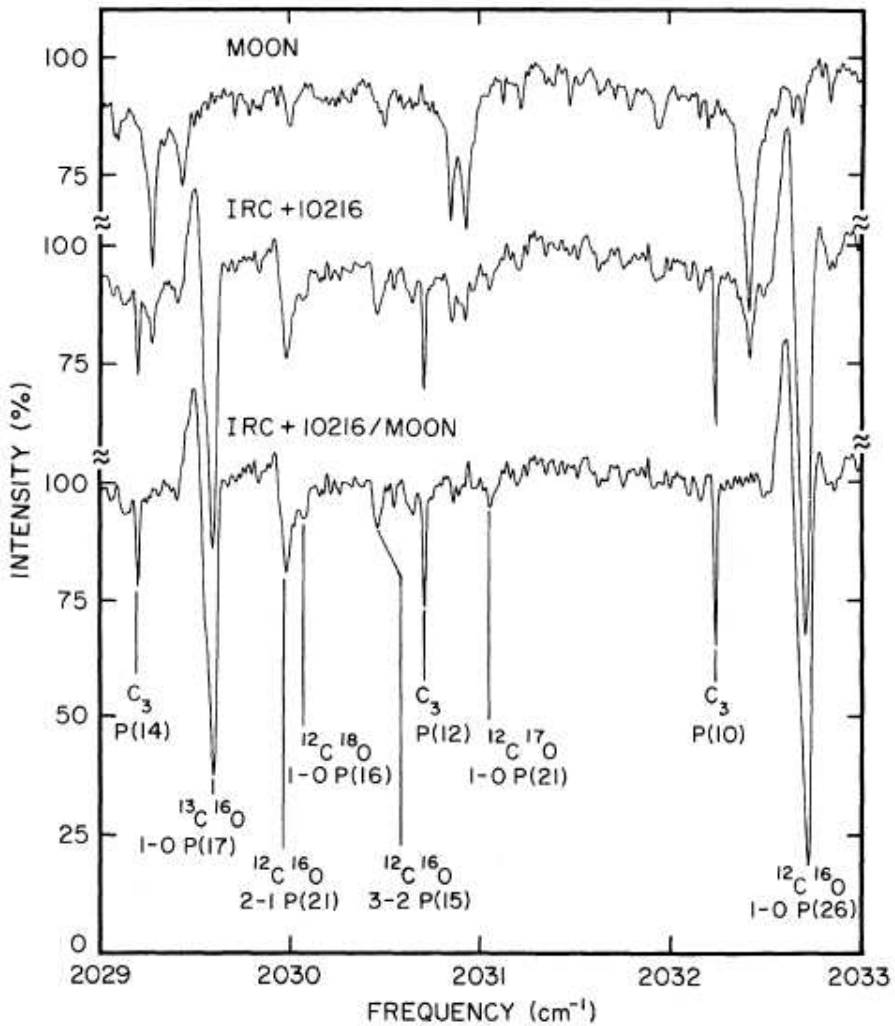

Vibration-rotation lines of C3 ν_2 in Sgr B2

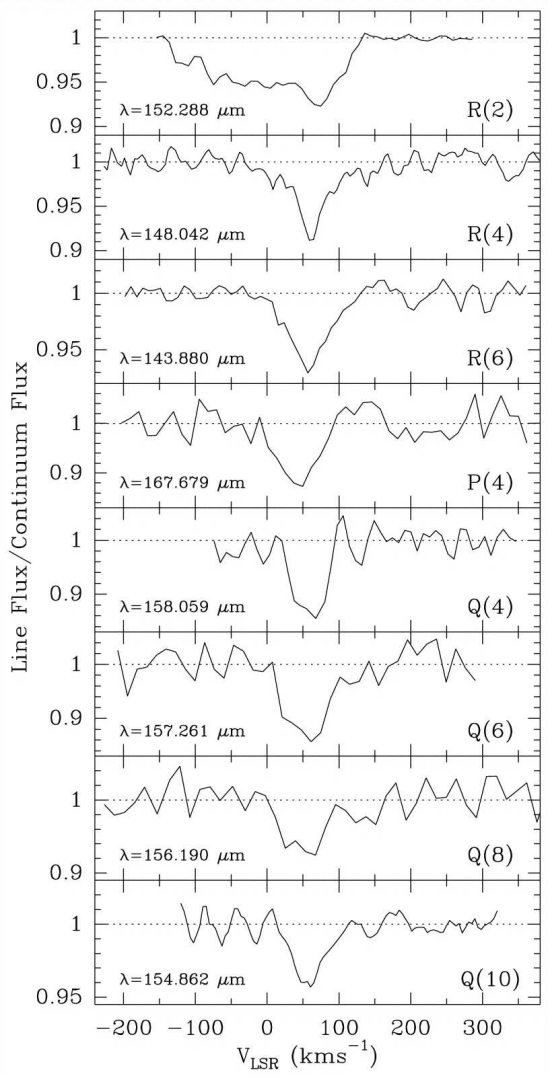

ISO LWS absorption lines towards Sgr B2 (Cernicharo, Goicoechea, & Caux 2000, 534L, 199). Also Herschel/HIFI observations of C_3 originating in the warm envelope of massive star forming regions (Mookerjea 2010, 2012).

Cometary system C3 around 4050 Å in diffuse clouds

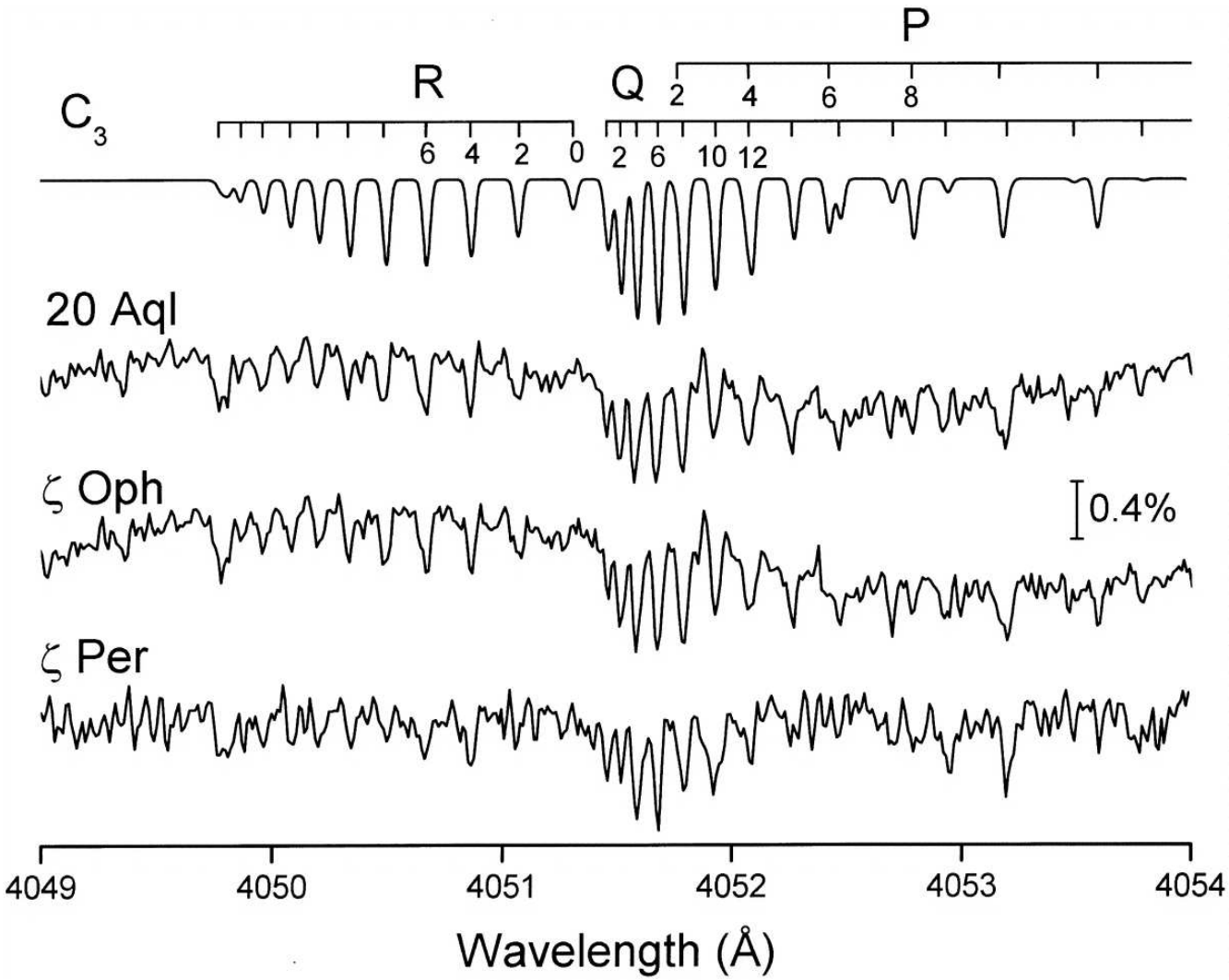

Maier et al. 2001 ApJ, 553, 267

Cometary system C3 around 4050 Å in diffuse clouds

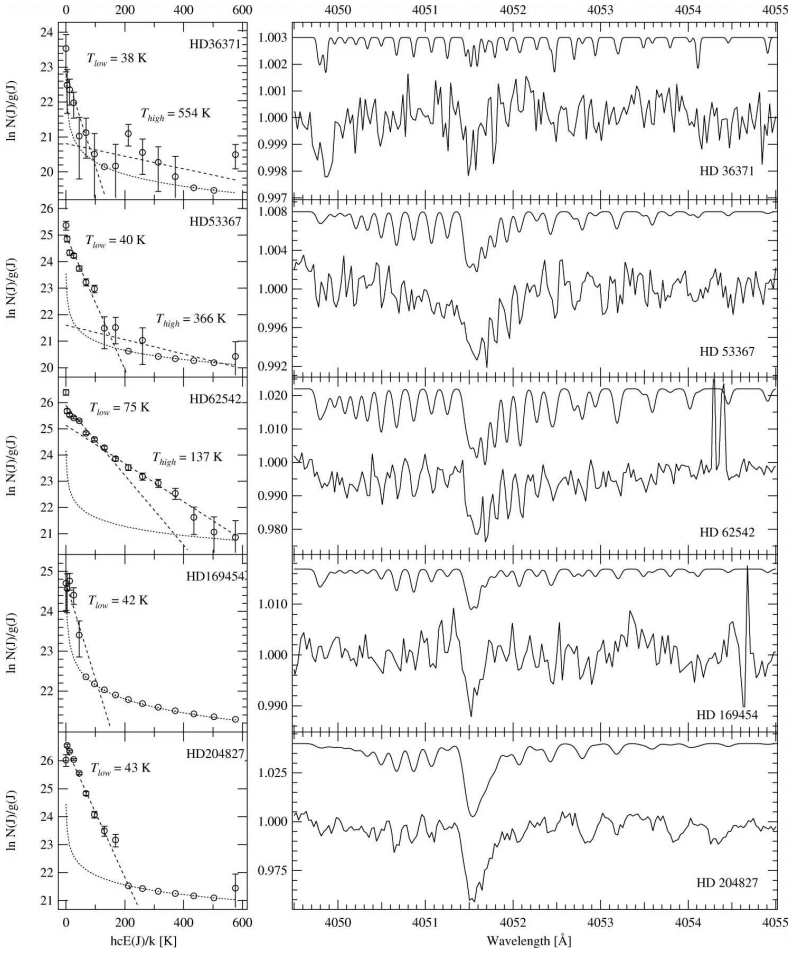

Adamkovics, Blake, & McCall 2003, ApJ, 595, 235

Monninger et al. 2002, J. Phys. Chem. A, 106, 5779

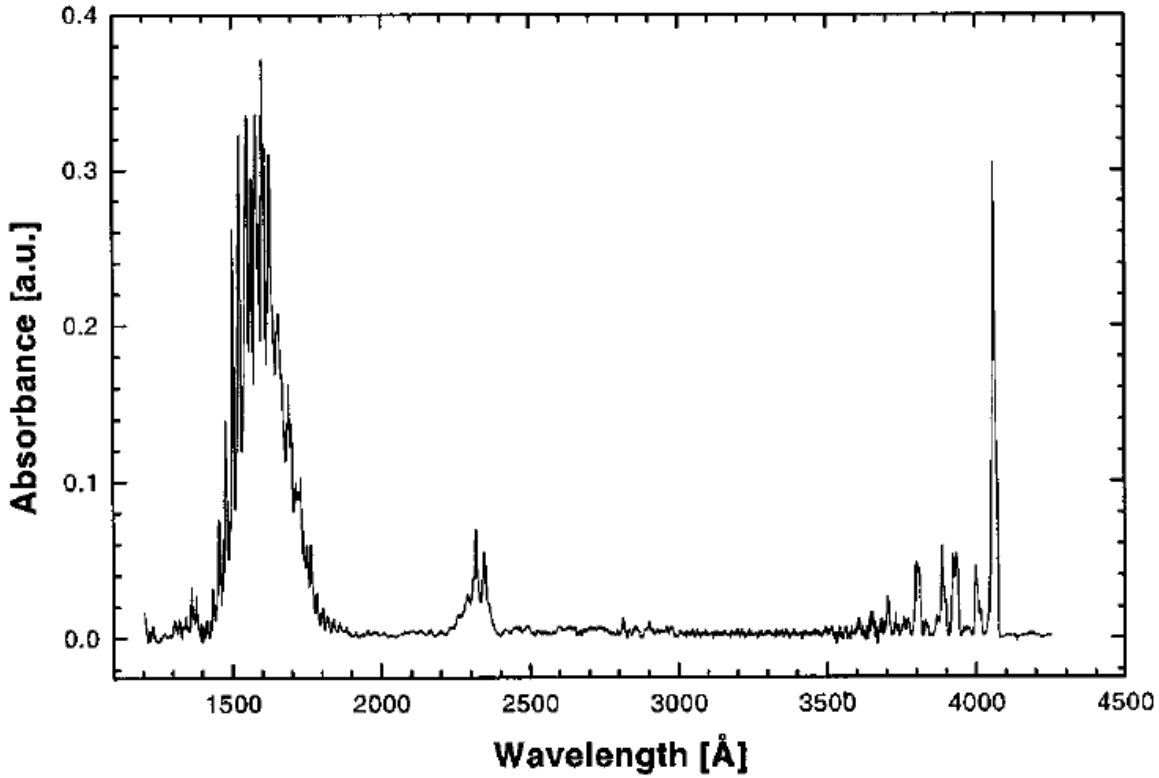

Electronic absorption spectrum of carbon vapor trapped in solid neon at 4.3 K in the vacuum ultraviolet-visible wavelength range. The two electronic transitions of C_3 at 1600 and 1700 Å are the dominant features.

Electronic structure of C3

State	T_e cm^{-1}	ω_1 cm^{-1}	ω_2 cm^{-1}	ω_3 cm^{-1}
$^1\Sigma_u^+$	~44000	1080.0	300.0	780.0
$^1\Delta_u/\Pi_g$	~34710	940.0	168.0	
$b^3\Pi_g^+$	?~26000		345.0	
$A^1\Pi_u$	25000	1089.9	311.1	563.0
$a^3\Pi_u^+$	17076	1154.2	505.0	1455.3
$X^1\Sigma_g^+$	0	1226.0	63.5	2040.0

Comments

- $A^1\Pi_u$–$X^1\Sigma_g^+$ - cometary system around 4050 Å
- $a^3\Pi_u^+$–$X^1\Sigma_g^+$ - weak emission at 5865 Å
- $^1\Sigma_u^+$–$X^1\Sigma_g^+$ - strong band around 1700 Å
- $a^3\Pi_u^+$ - metastable level (lifetime about 20 ms)

Laboratory experiment

Laboratory spectra of C_3 are recorded in direct absorption using cavity ring-down laser spectroscopy. In the experiment, supersonically jet-cooled C_3 radicals are produced in a pulsed (10 Hz) planar plasma expansion generated by discharging 0.5% C_2H_2 diluted in a 1:1 helium/argon gas mixture. A 3 cm $\times$ 300 μm slit discharge nozzle is employed to generate a planar plasma expansion which provides an essentially Doppler-free environment and a relatively long effective absorption path length. The rotational temperature of C_3 in the plasma jet is estimated at 30 K.

Laboratory data

- The wavelength accuracy of better than 0.01 Å is achieved in the final laboratory spectrum, except for the $02^+0 - 000$ band at $\sim$3916 Å, where the line position of the strongest C_3 transition, i.e. Q(4) line at 3916.05 Å, in the astronomical spectrum towards HD 169454. This yields an absolute wavelength accuracy of $\sim$0.05 Å for the $02^+0 - 000$ band, while the accuracy of relative line positions within this band is better than 0.01 Å.
- the absolute line intensities in the recorded spectrum may be underestimated, due to a specific linewidth effect associated with the cavity ring-down technique, hence in the analysis the theoretical rotational strengths are used

Observational material

The observational material was obtained using the UVES spectrograph mounted on the ESO Very Large Telescope at Paranal (Chile) with resolution $R = 80,000$ in the blue arm (3020 – 4980 Å) occupying the C_3 **bands** of interest, as well as CH and CH^+. The spectra, averaged over 10 - 50 exposures are of exceptionally high S/N ratio with values between 1900-2800.

Spectrum of A-X 000-000 in sight line to HD 169454

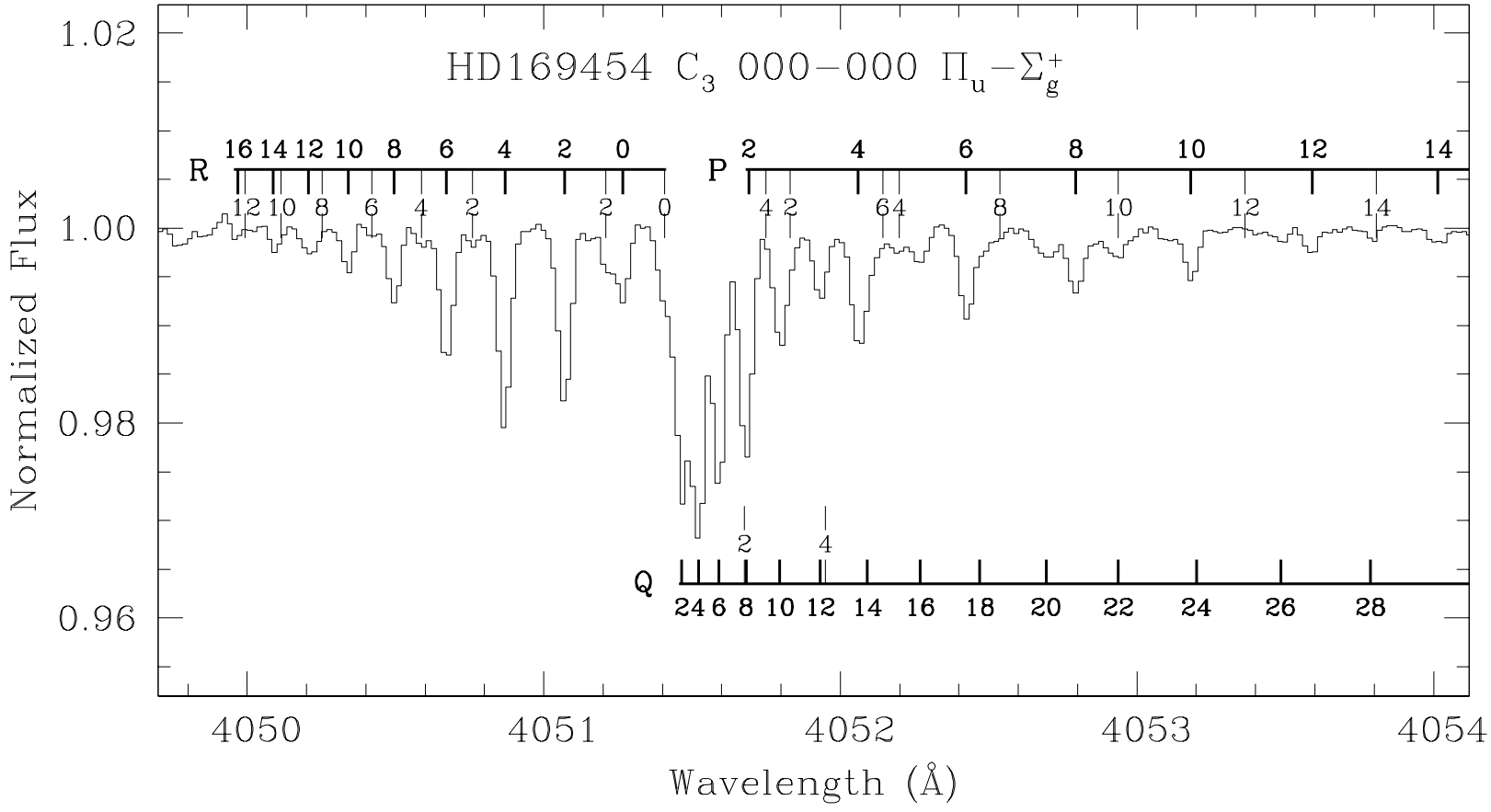

Positions of rotational lines are marked with thick lines. Thin line tags mark perturbed rotational lines (Zhang et al. 2005).

Spectrum of A-X 100–000 band in sightline to HD 169454

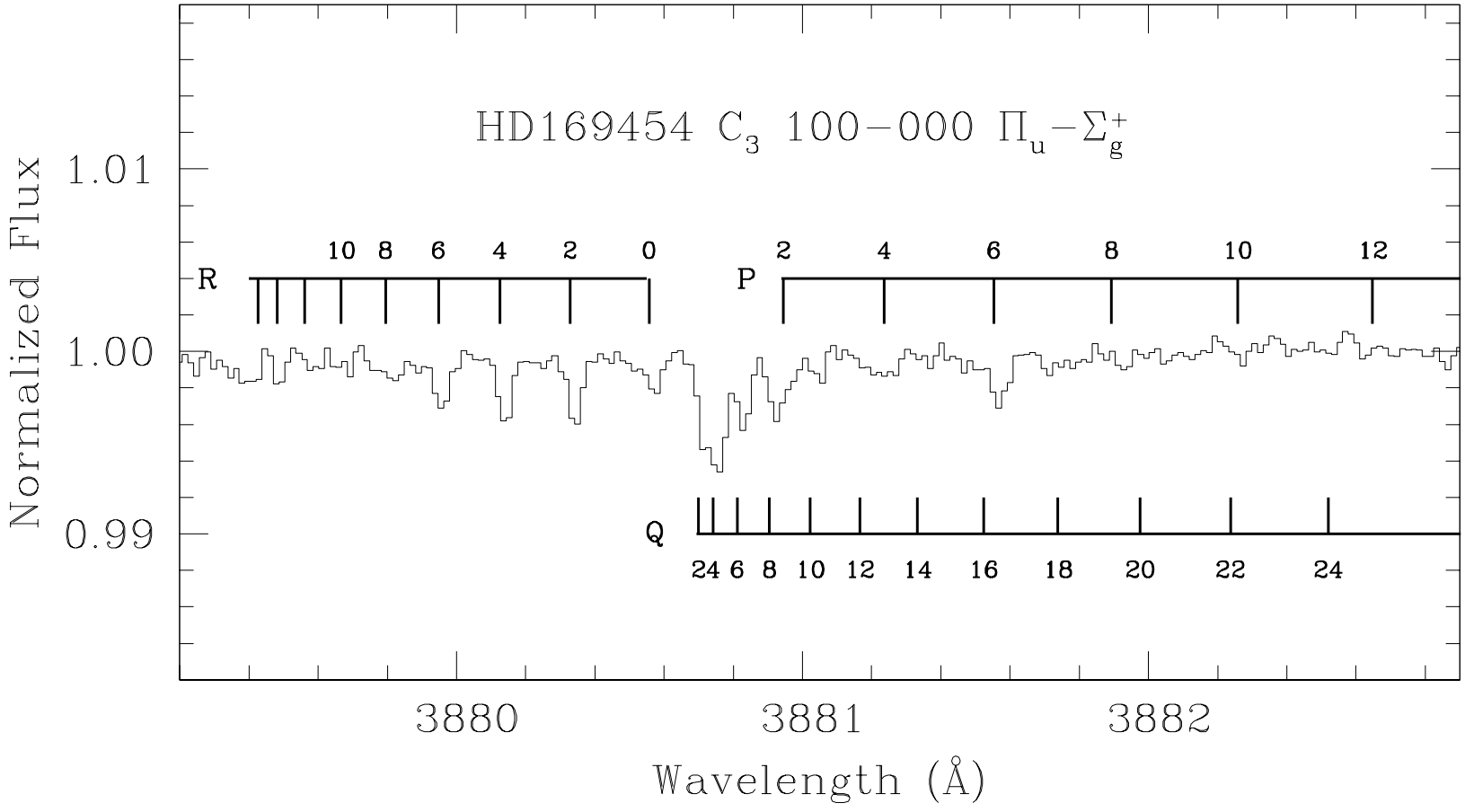

Positions of rotational lines are marked with thick lines.

Spectrum of A-X 002–000 band in sightline to HD 169454

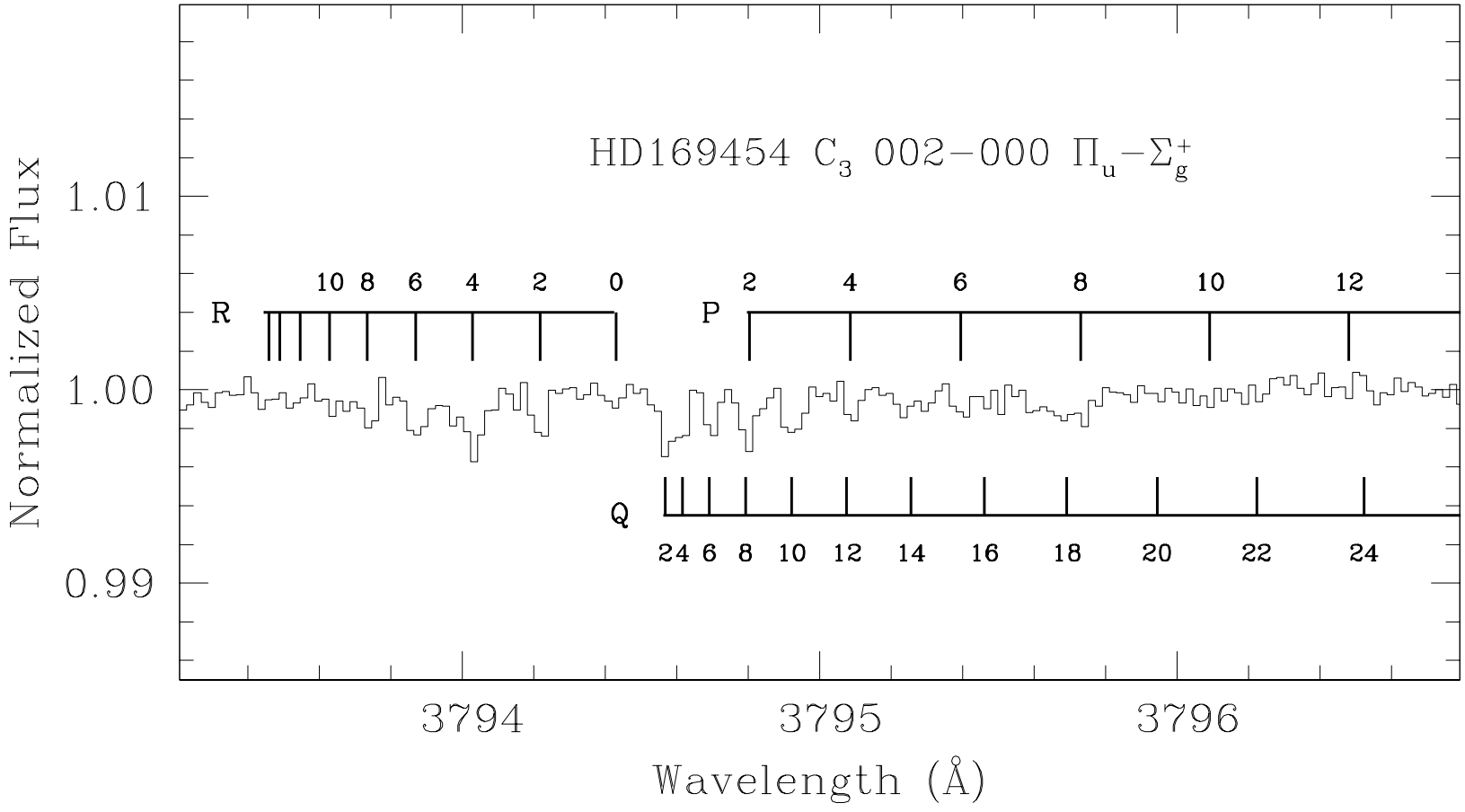

Positions of rotational lines are marked with thick lines.

Spectrum of A-X 02-0–000 band in sightline to HD 169454

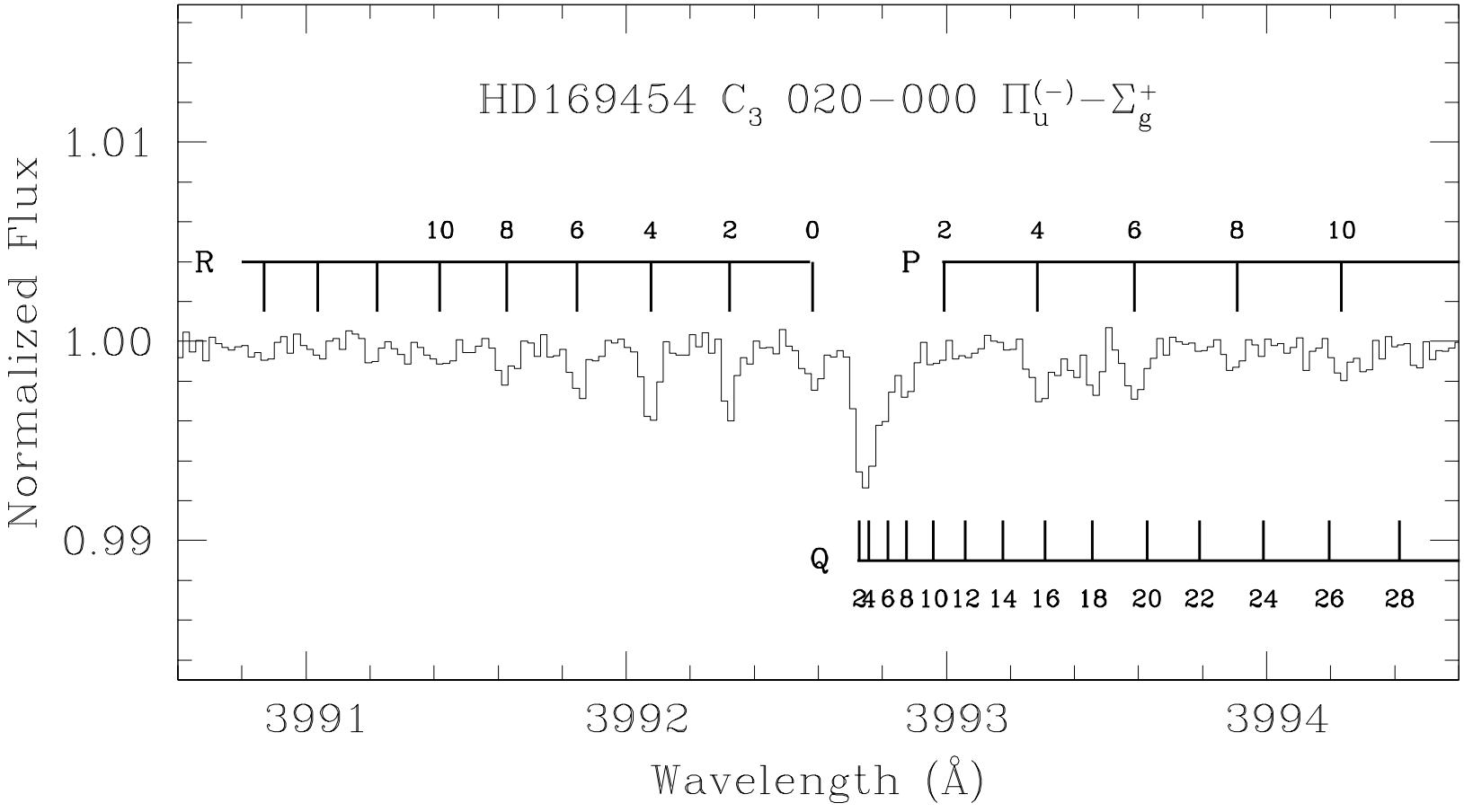

Positions of rotational lines are marked with thick lines.

Spectrum of A-X 02+0–000 band in sightline to HD 169454

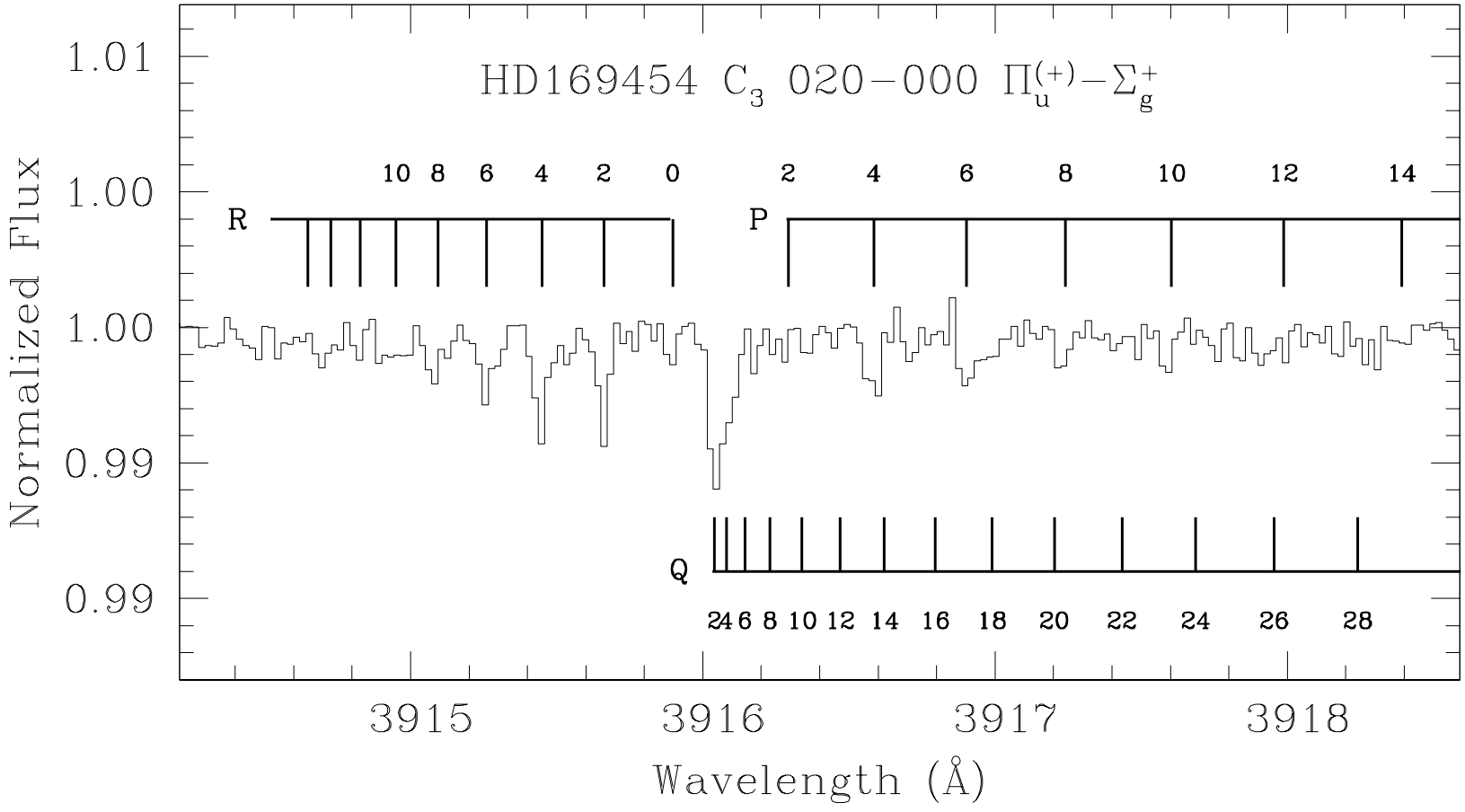

Positions of rotational lines are marked with thick lines.

Spectrum of A-X 04-0–000 band in sightline to HD 169454

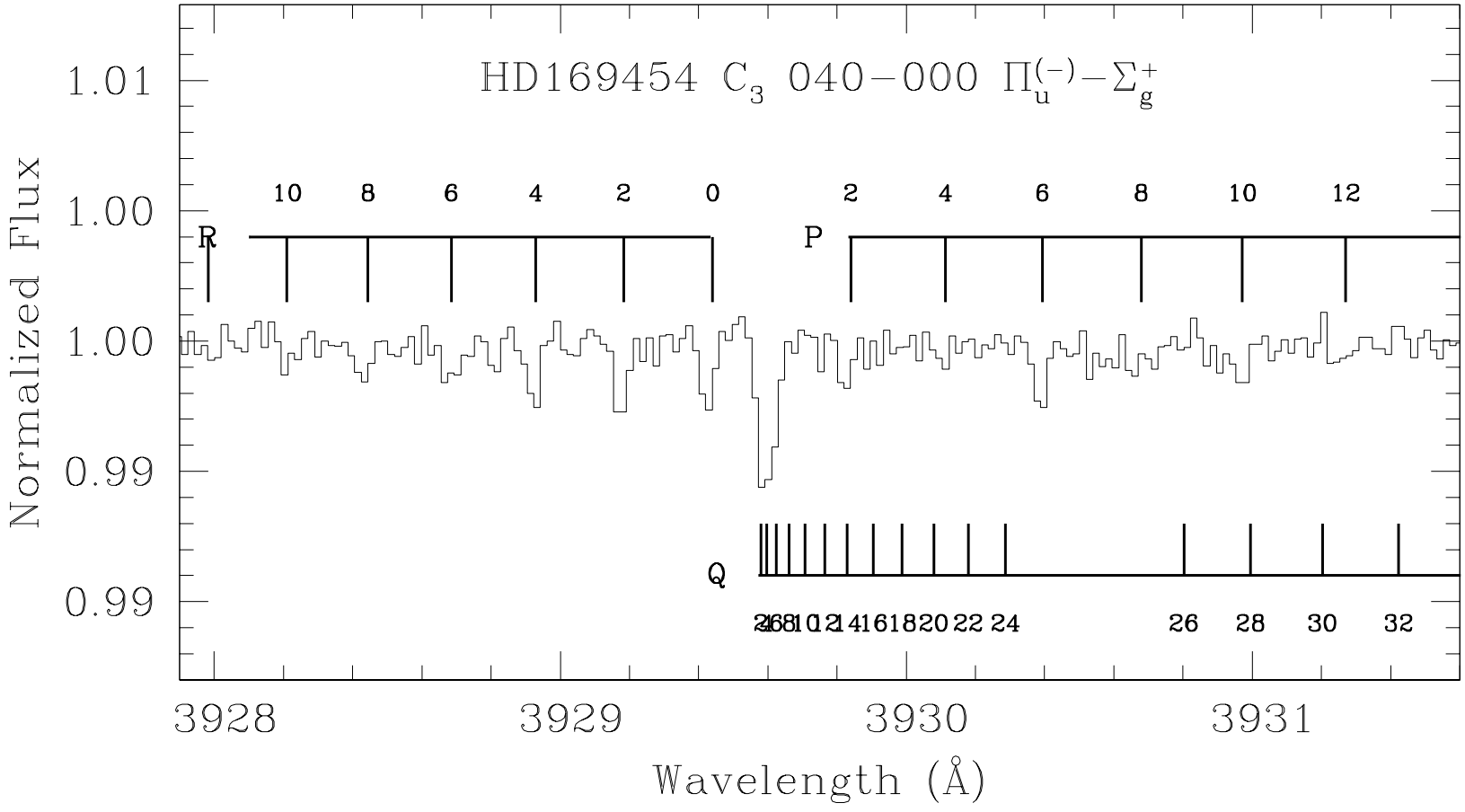

Positions of rotational lines are marked with thick lines.

Spectrum of A-X 04+0–000 band in sightline to HD 169454

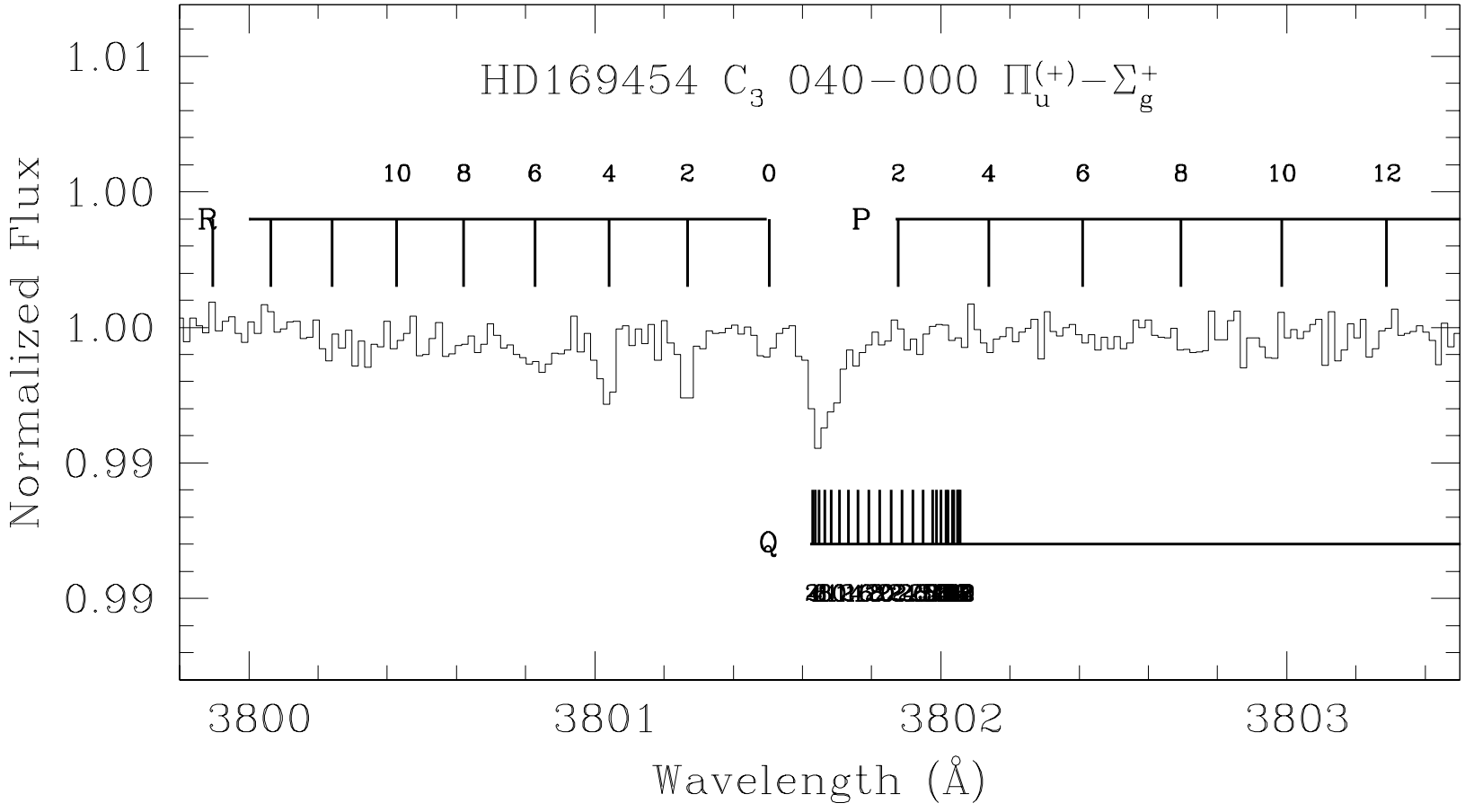

Positions of rotational lines are marked with thick lines.

Spectrum of A-X 12-0–000 band in sightline to HD 169454

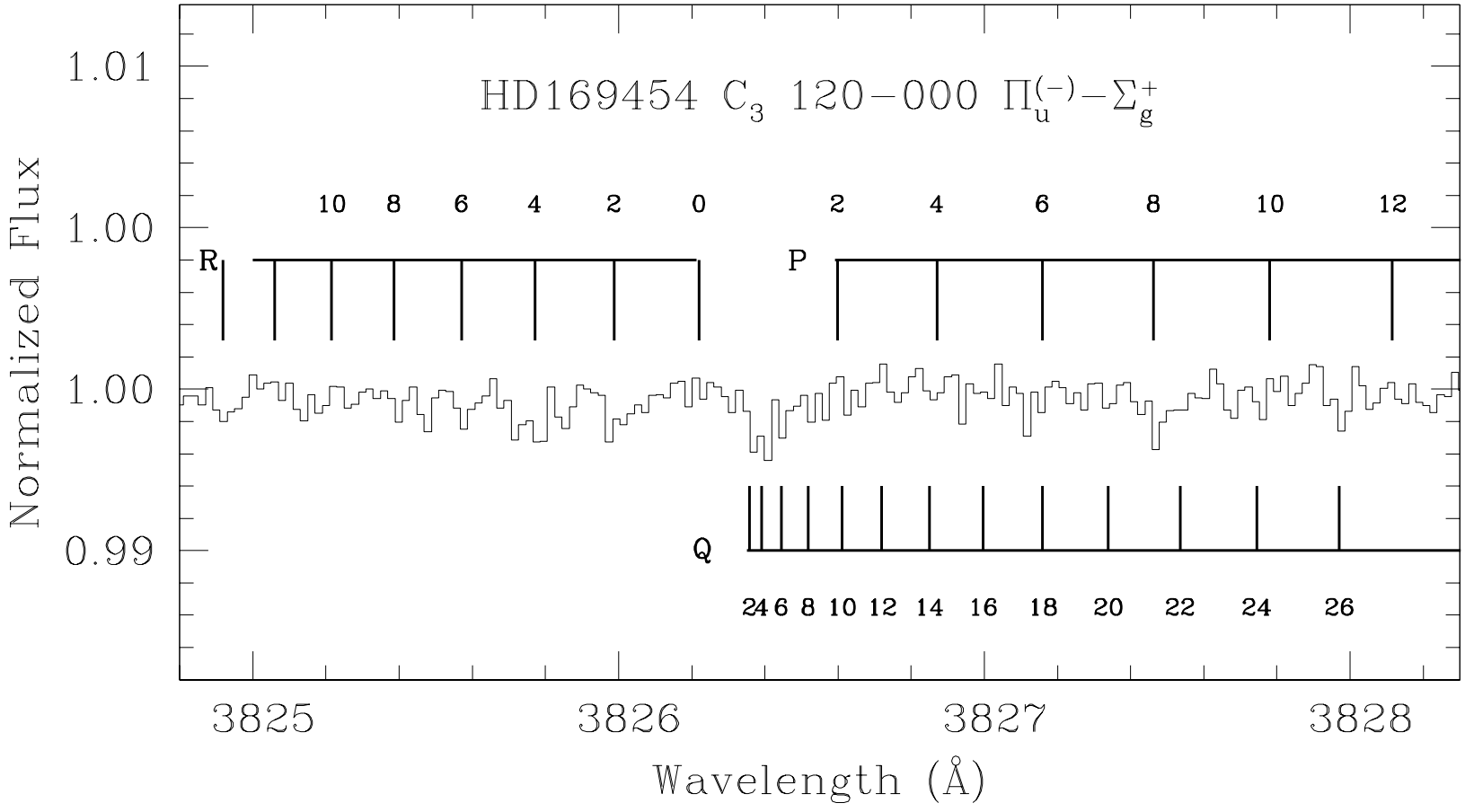

Positions of rotational lines are marked with thick lines.

- earlier finding list of different bands: Zhang et al. (2010) (000-000 including perturbations) Chen et al. (2010), Gausset et al. (1963)
- electronic transition moment f_{el}=0.0246 (Becker 1979)
- Franck-Condon factors of 000-000 transition 0.746 from Radic (1977)
- Honl-London factors - standard formula for J,K
- perturbative approach - Honl-London factors for 000-000 - diagonalization of experimental hamiltonian of Zhang et al. (2010)

Franck-Condon factors of the analysed vibronic bands.

Origin (Å)	Band	FC			References
		J&M	R-P	this work	
4051.6	000 Π_u	0.594	0.741	0.741	1,2
3880.7	100 Π_u			0.13±0.02	2
3992.8	02^-0 Π_u	0.087	0.170	0.14±0.03	3
3916.0	02^+0 Π_u	0.081	0.170	0.14±0.03	2
3929.5	04^-0 Π_u	0.083	0.056	0.10±0.03	2
3801.7	04^+0 Π_u	0.048	0.056	0.10±0.03	4
3794.2	002 Π_u			0.08±0.02	4
3826.0	12^-0 Π_u			0.04±0.01	2,5

Spectrum of A-X 000-000 in sight line to HD 169454

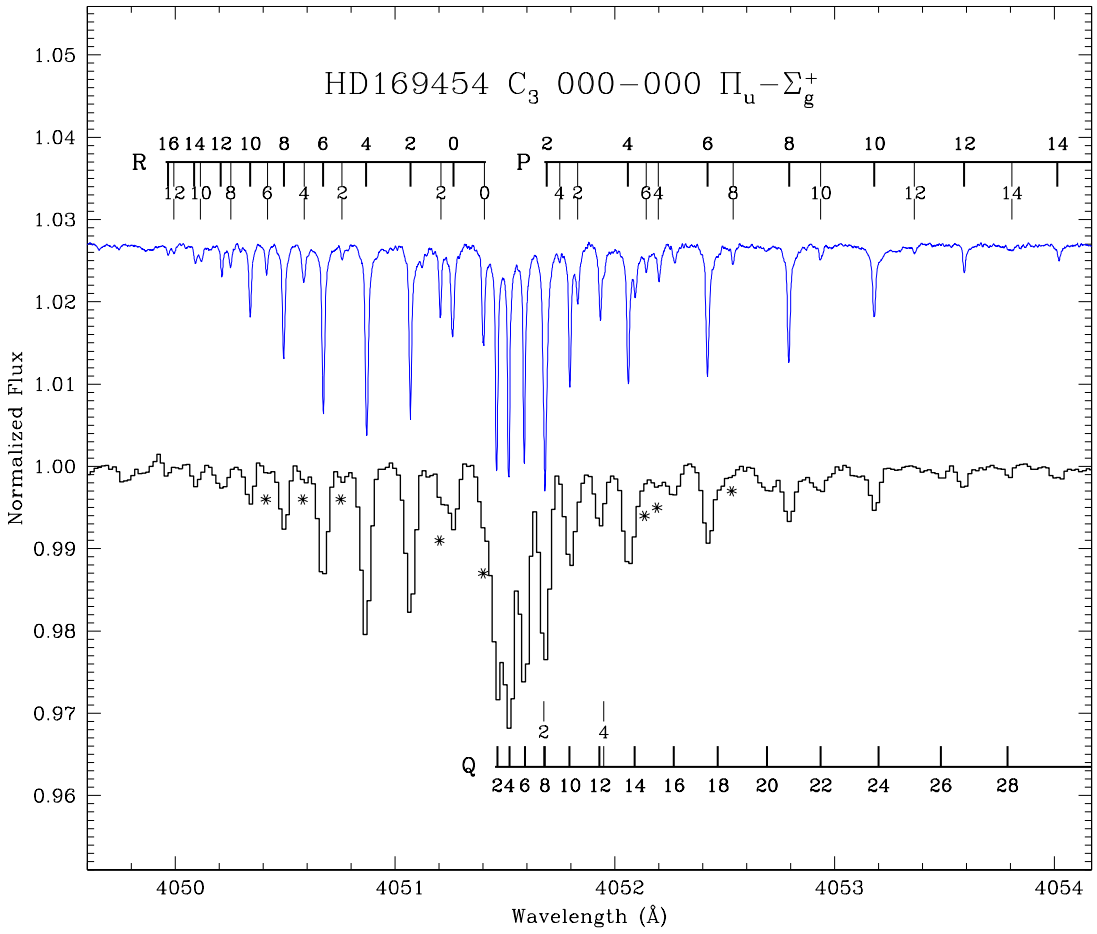

Positions of rotational lines are marked with thick lines. Thin line tags mark perturbed rotational lines (Zhang et al. 2005).

Laboratory Spectrum of A-X 000-000 (Zhang et al. 2005)

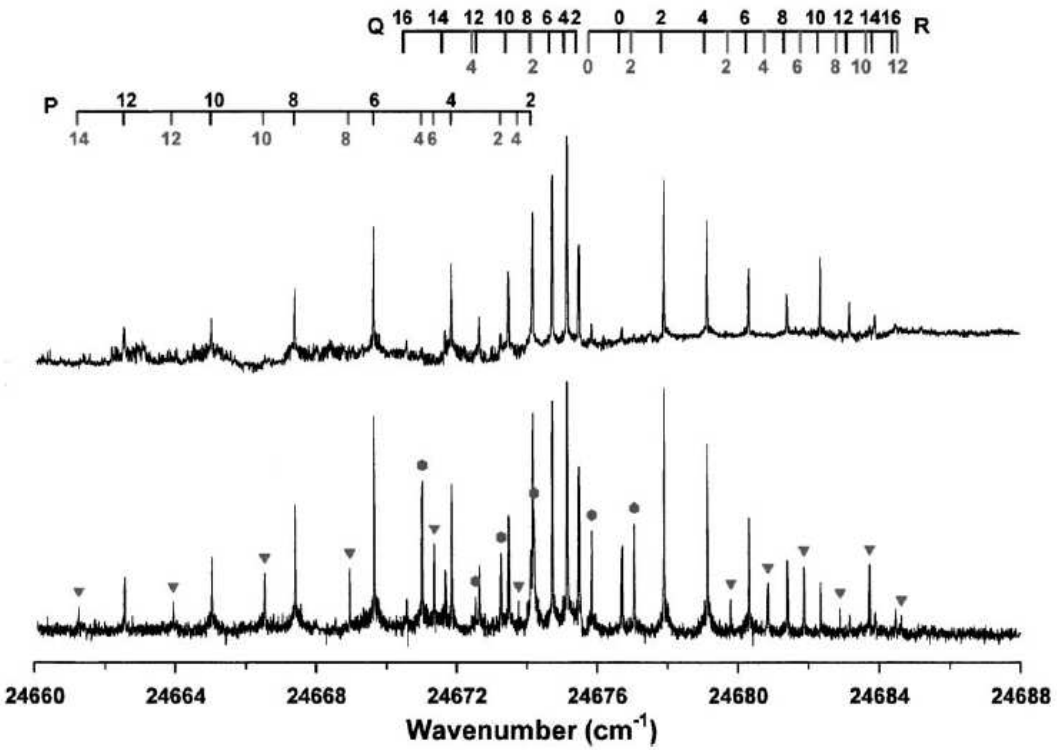

Excitation spectra (LIF) of $A^1\Pi_u$-$X^1\Sigma_g$ recorded at two different gatings: 20-150 ns (upper trace), 800-2300 (lower trace). Positions of perturbed rotational lines are marked with triangles (triplet state) and hexagons (P=1)

Laboratory Spectrum of A-X 000-000 (Zhang et al. 2005)

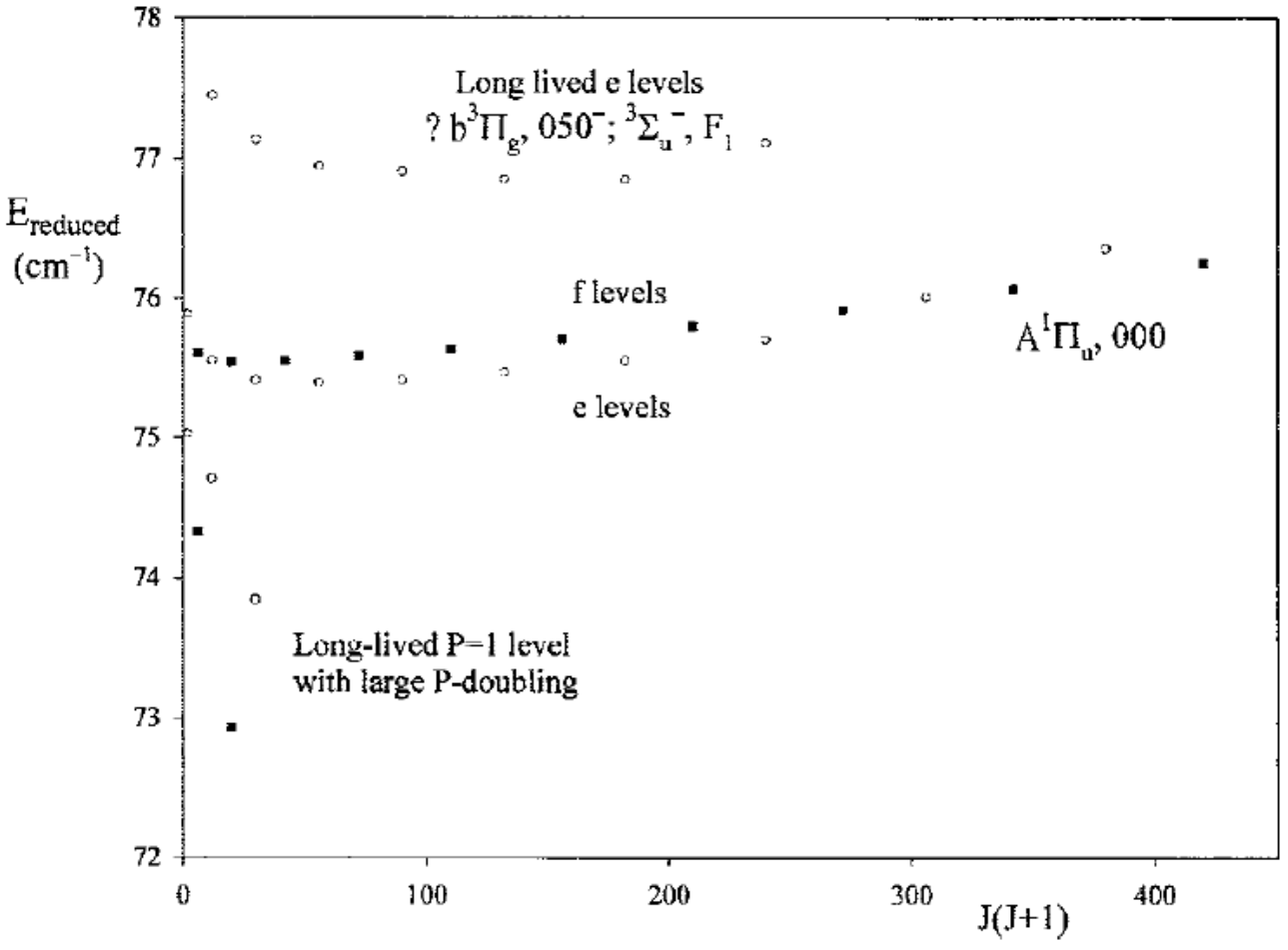

Laboratory Spectrum of A-X 000-000 (Zhang et al. 2005)

TABLE IV. Matrices for a deperturbation of the rotational level structure of the $\tilde{A}\,^1\Pi_u$, 000 state of C_3 and its perturbing states. There are two matrices, one for e parity and one for f parity. The e parity matrix is of order 4, as shown; the f parity matrix, of order 3, is obtained by striking out the last row and column. The upper and lower signs refer to the f and e parity matrices, respectively. A case (a) basis has been assumed for the $^3\Sigma^-$ state.

	$\lvert\tilde{A}\,^1\Pi_u, f/e\rangle$	$\lvert P=1, f/e\rangle$	$\lvert{}^3\Sigma^-_{1u}, f/e\rangle$	$\lvert{}^3\Sigma^-_{0u}, e\rangle$
$\langle\tilde{A}\,^1\Pi_u, f/e\rvert$	$T_0^\Pi + (B^\Pi \pm q^\Pi/2)J(J+1) - D^\Pi J^2(J+1)^2$	a	ξ	0
$\langle P=1, f/e\rvert$		$T_0^P + B^P J(J+1) \pm (q^P/2)J(J+1)$	0	0
$\langle{}^3\Sigma^-_{1u}, f/e\rvert$			$T_0^\Sigma + B^\Sigma J(J+1) + (2/3)\lambda - \gamma$	$-(2B^\Sigma - \gamma)[J(J+1)]^{1/2}$
$\langle{}^3\Sigma^-_{0u}, e\rvert$	symmetric			$T_0^\Sigma + B^\Sigma[J(J+1)+2] - (4/3)\lambda - 2\gamma$

Spectrum of A-X 000-000 in sight line to HD 169454

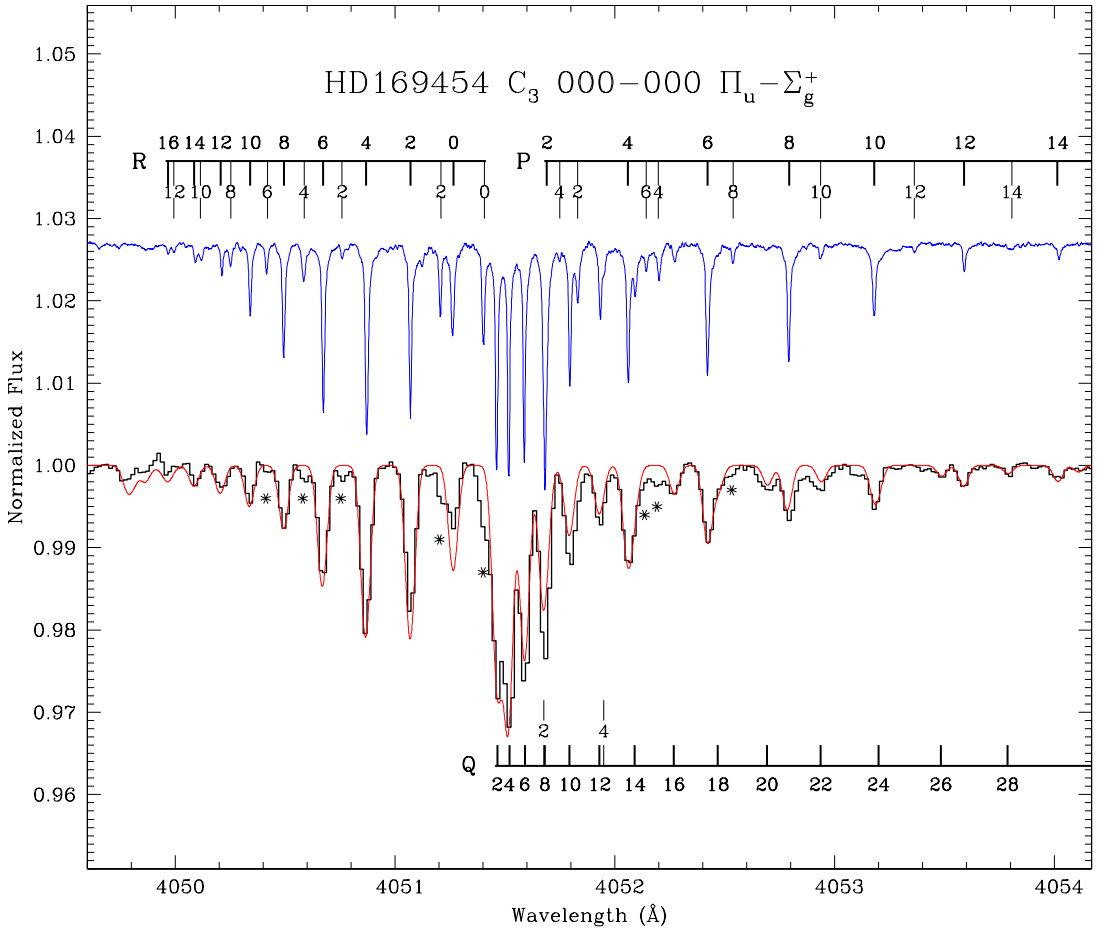

The fit (red line) using unperturbed line strengths.

Spectrum of A-X 000-000 in sight line to HD 169454

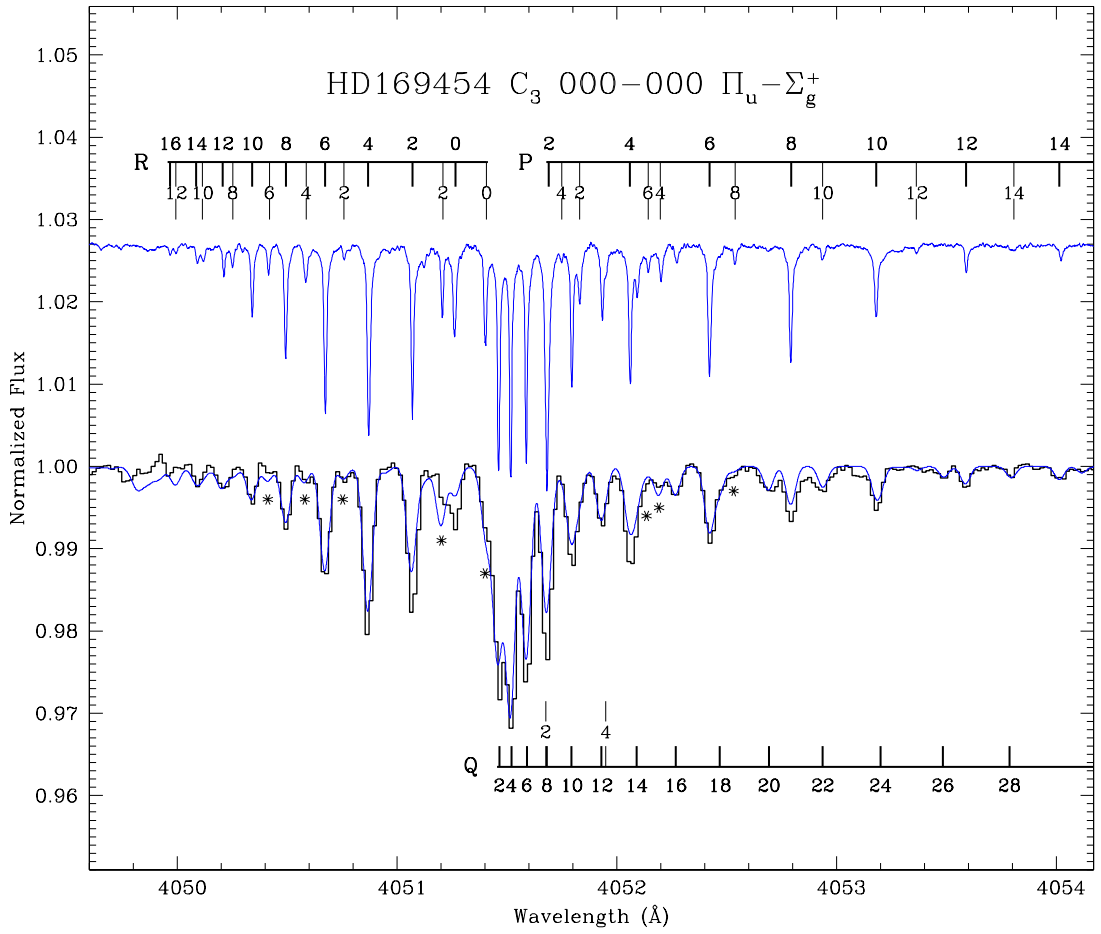

The fit (blue line) using perturbed line strengths.

Spectrum of A-X 000-000 in sight line to HD 169454

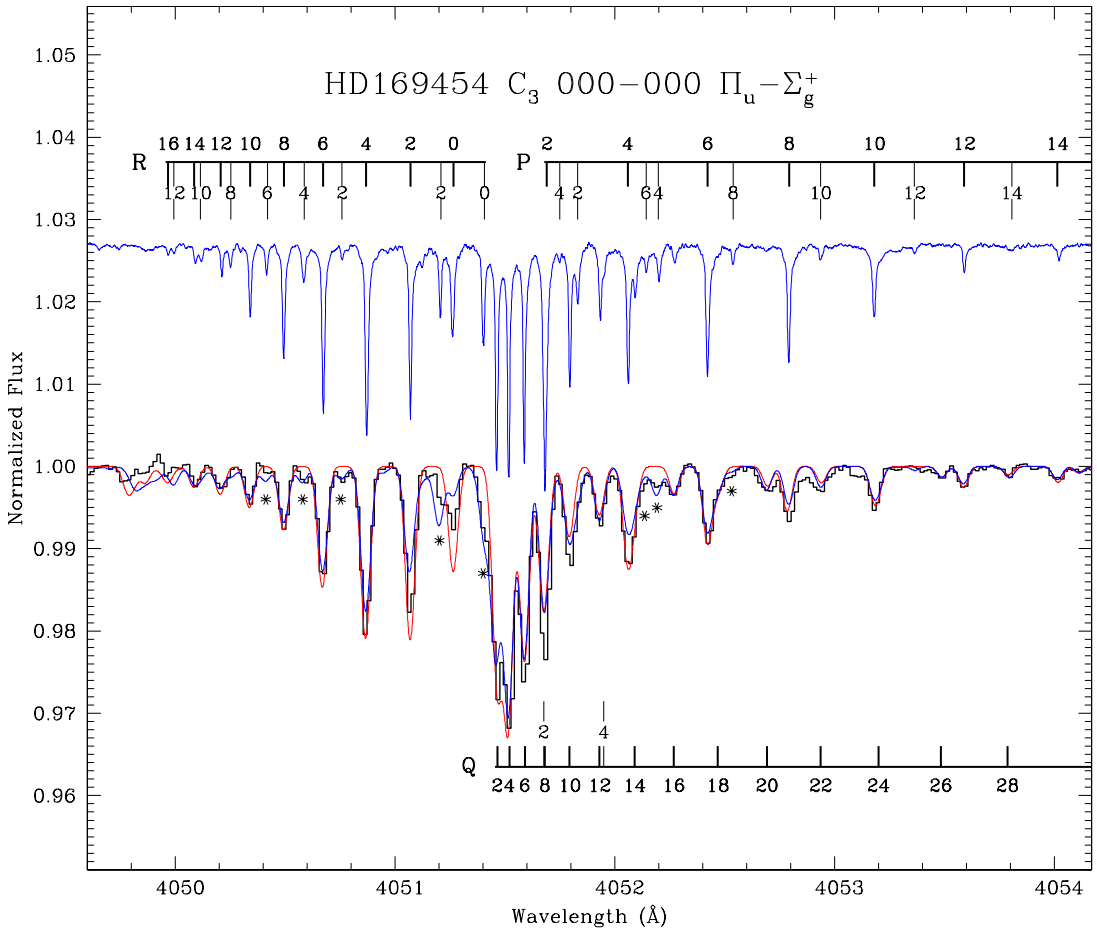

The fit using (blue line - perturbed, red line uperturbed) line strengths.

Spectrum of A-X 100–000 band in sightline to HD 169454

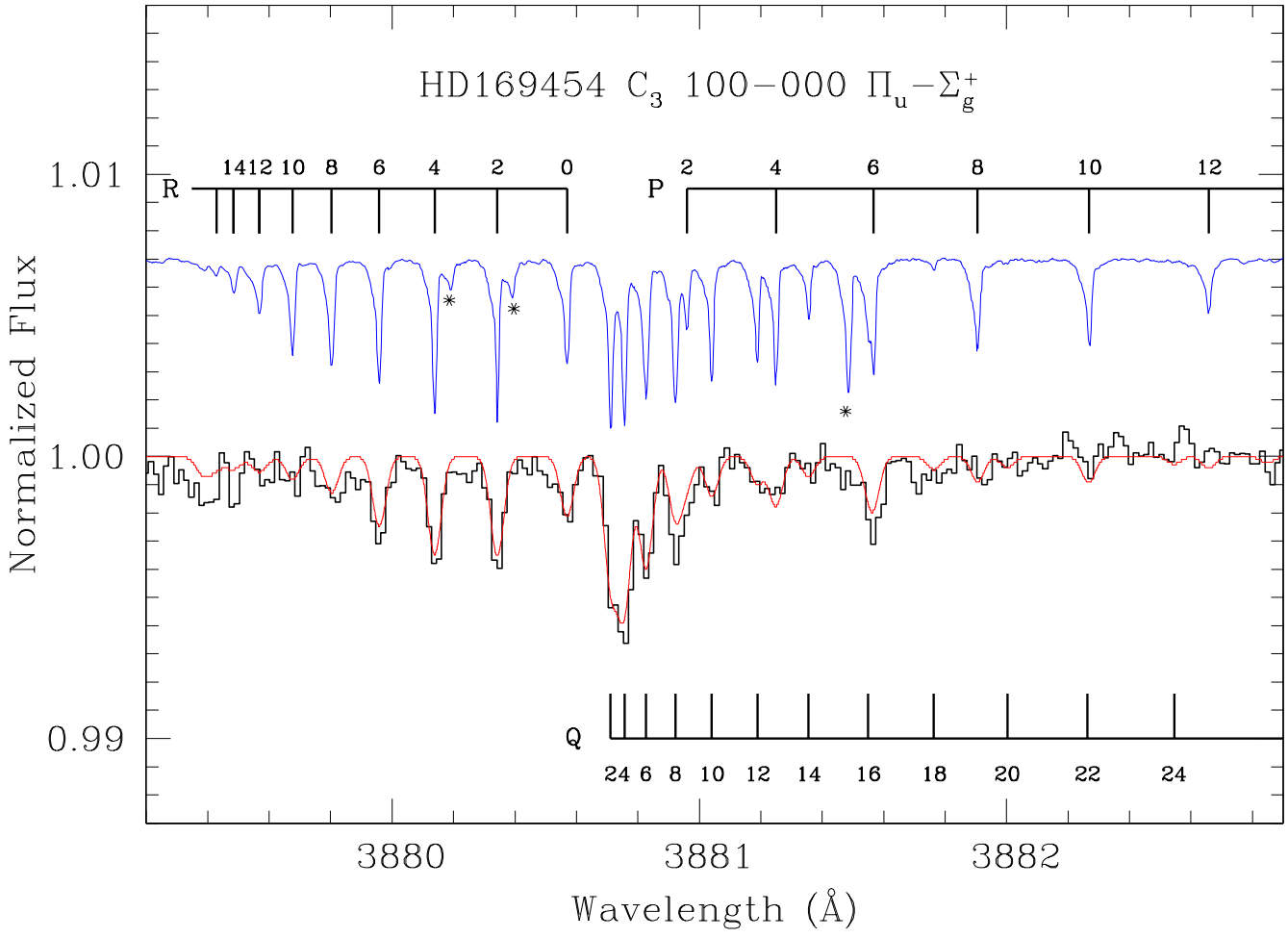

Positions of rotational lines are marked with thick lines.

Spectrum of A-X 002–000 band in sightline to HD 169454

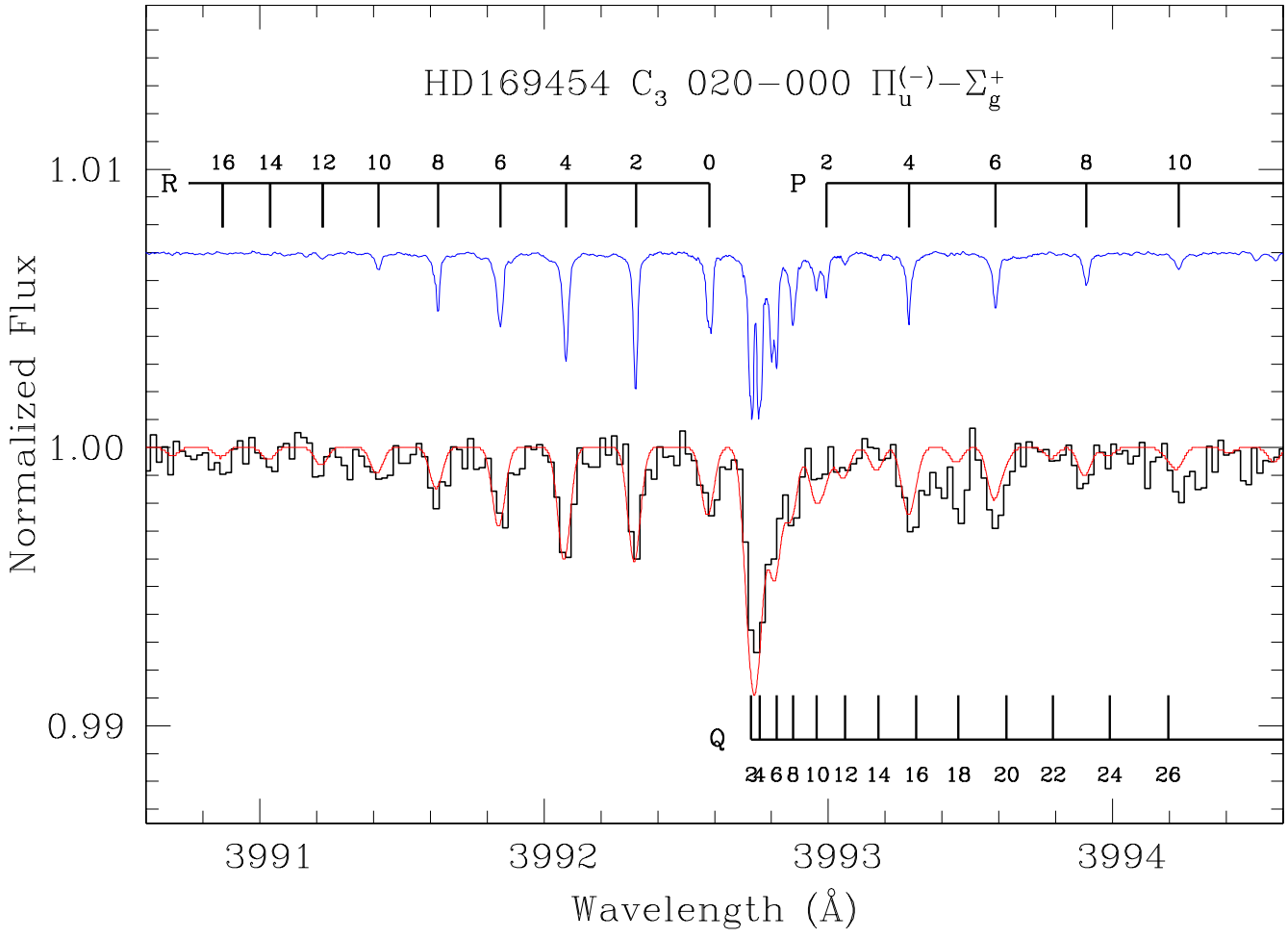

Positions of rotational lines are marked with thick lines.

Spectrum of A-X 02-0–000 band in sightline to HD 169454

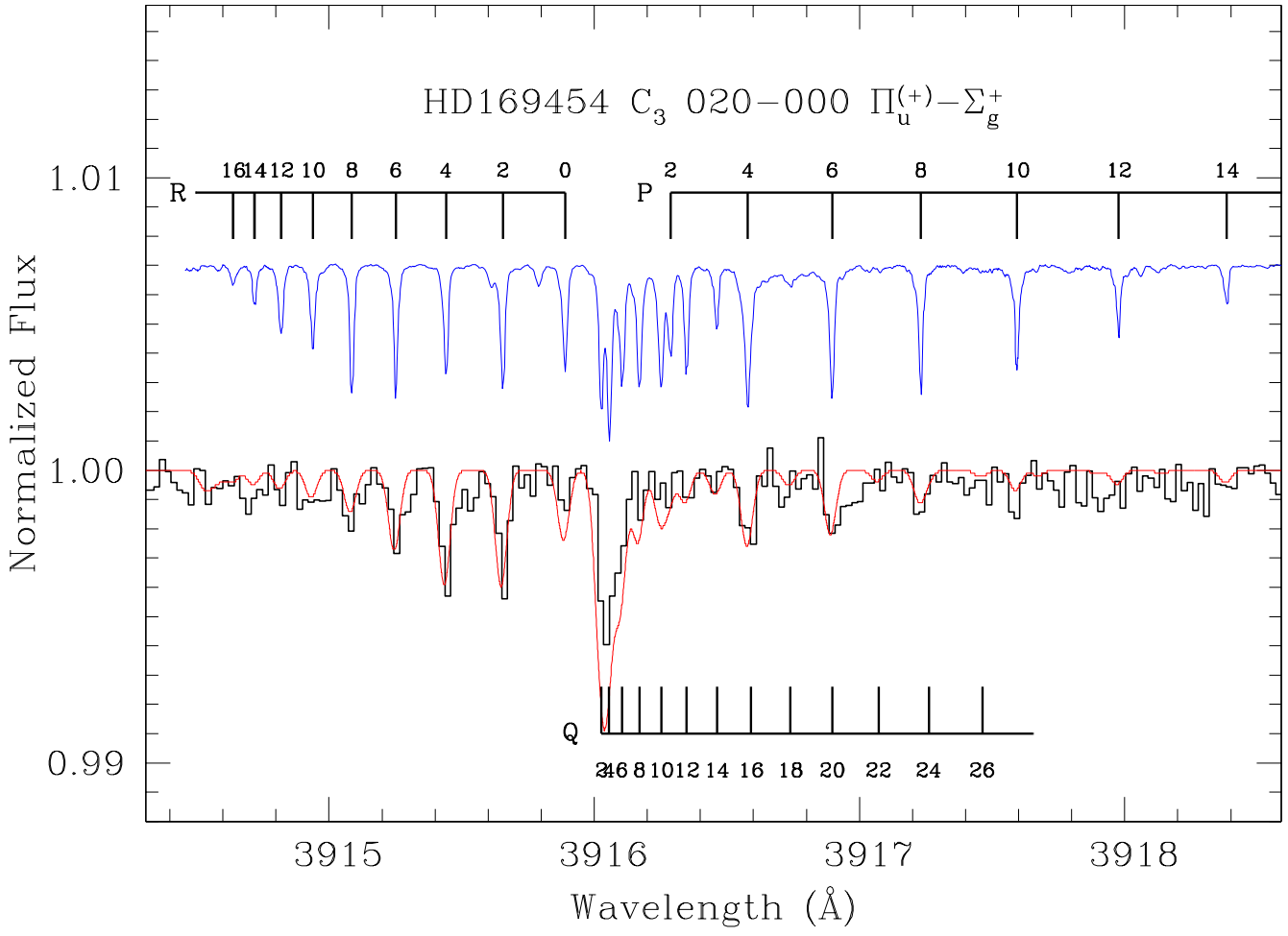

Positions of rotational lines are marked with thick lines.

Spectrum of A-X 02+0–000 band in sightline to HD 169454

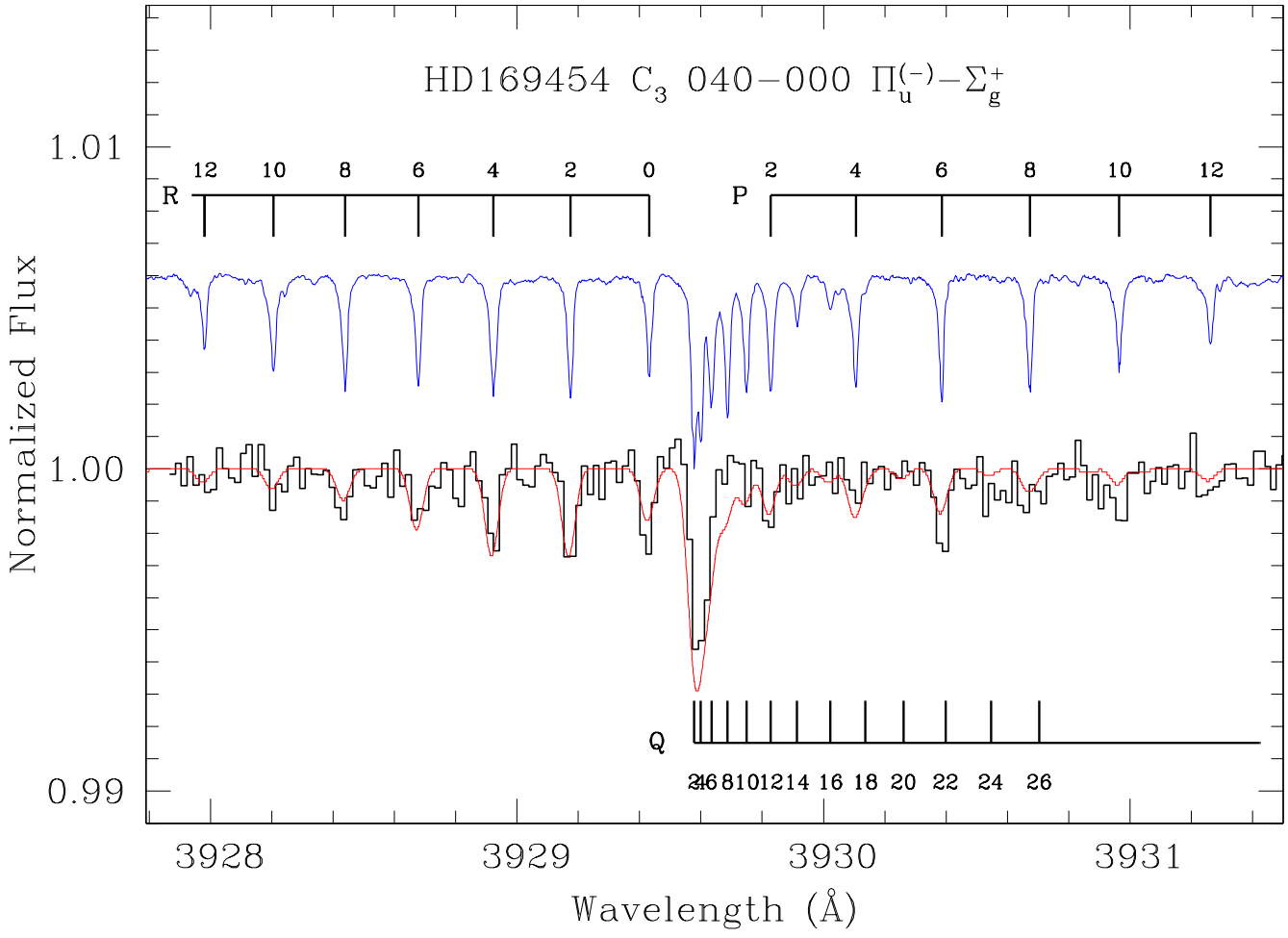

Positions of rotational lines are marked with thick lines.

Spectrum of A-X 04-0–000 band in sightline to HD 169454

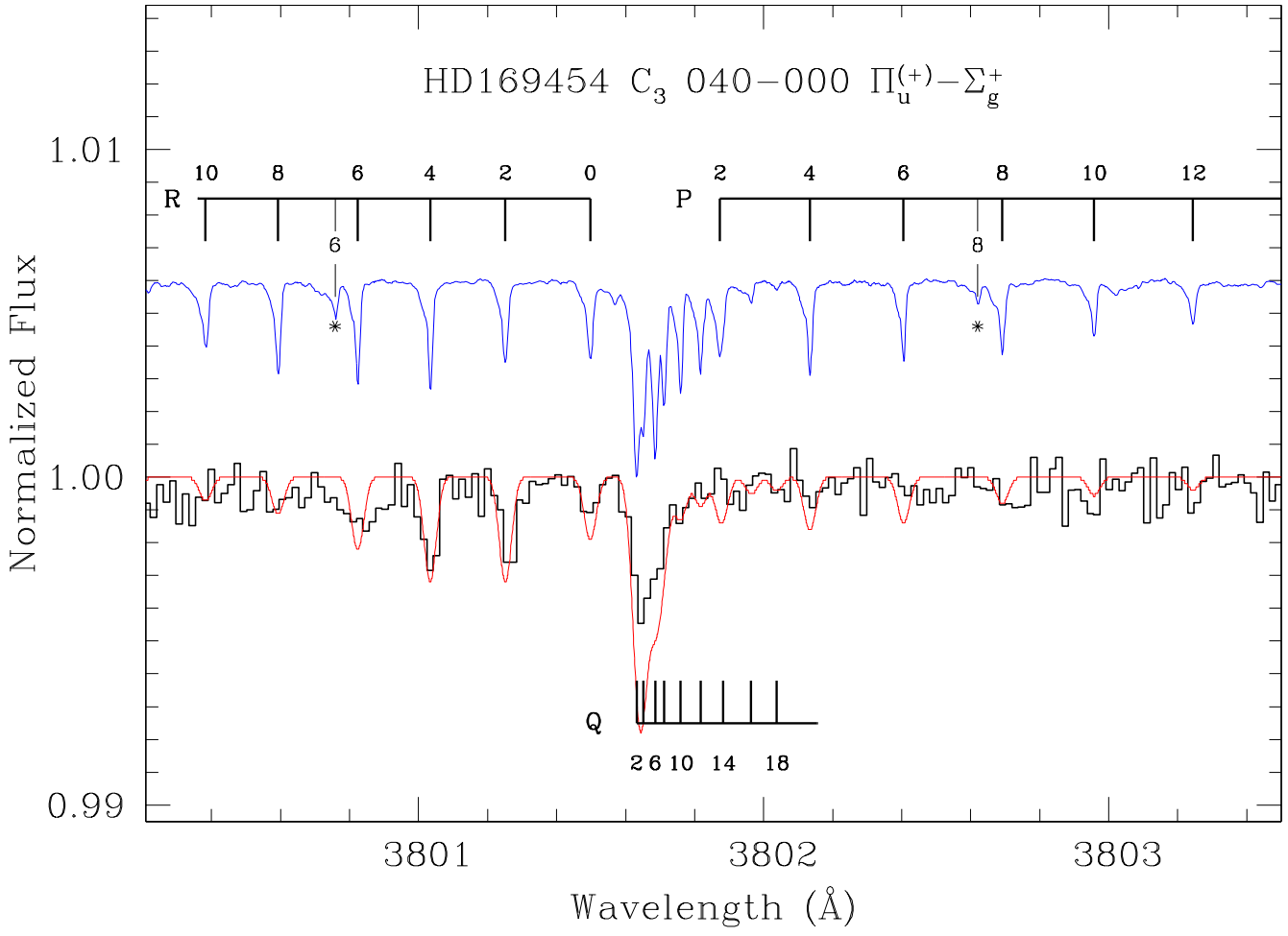

Positions of rotational lines are marked with thick lines.

Spectrum of A-X 04+0–000 band in sightline to HD 169454

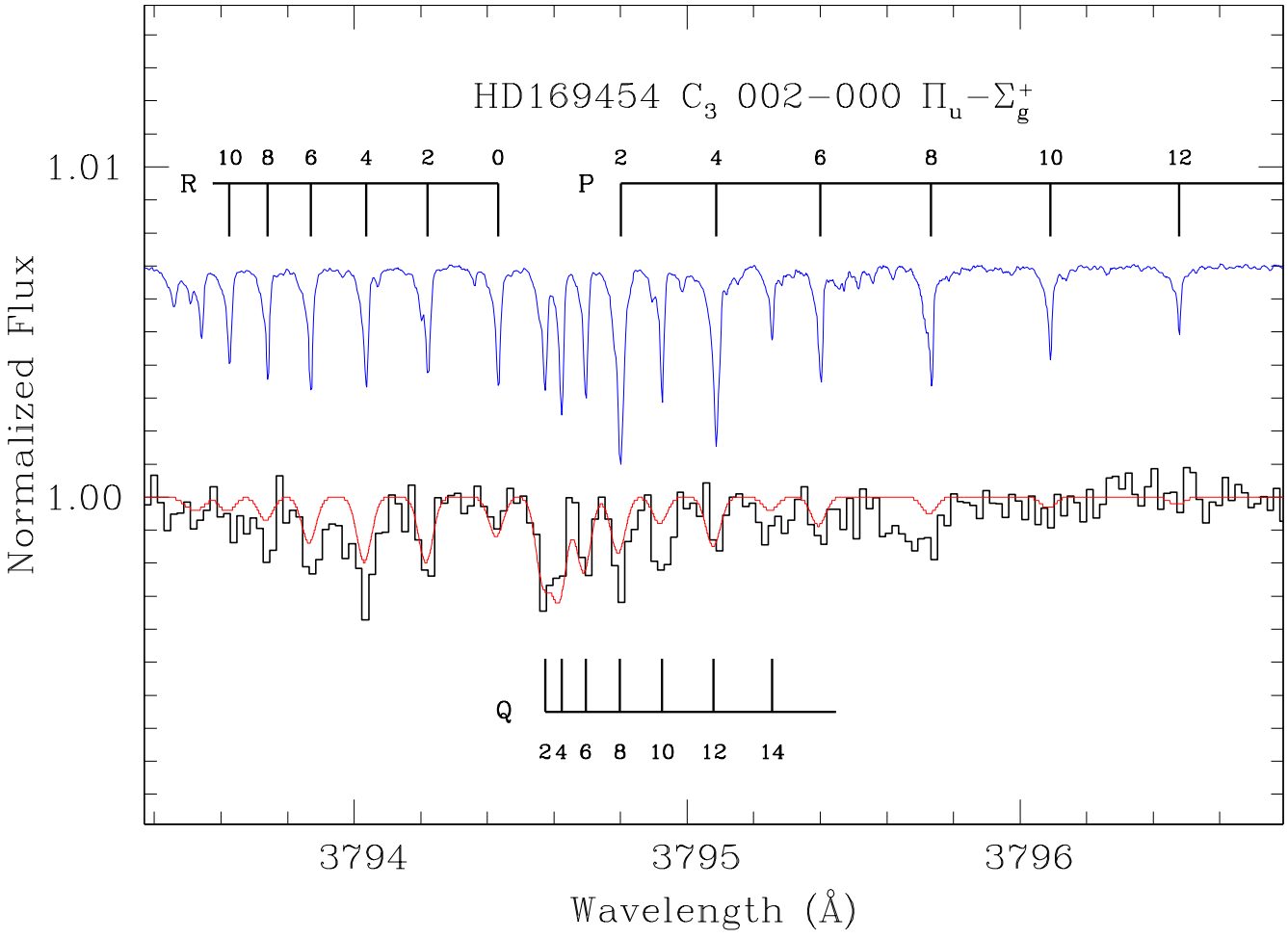

Positions of rotational lines are marked with thick lines.

Spectrum of A-X 12-0–000 band in sightline to HD 169454

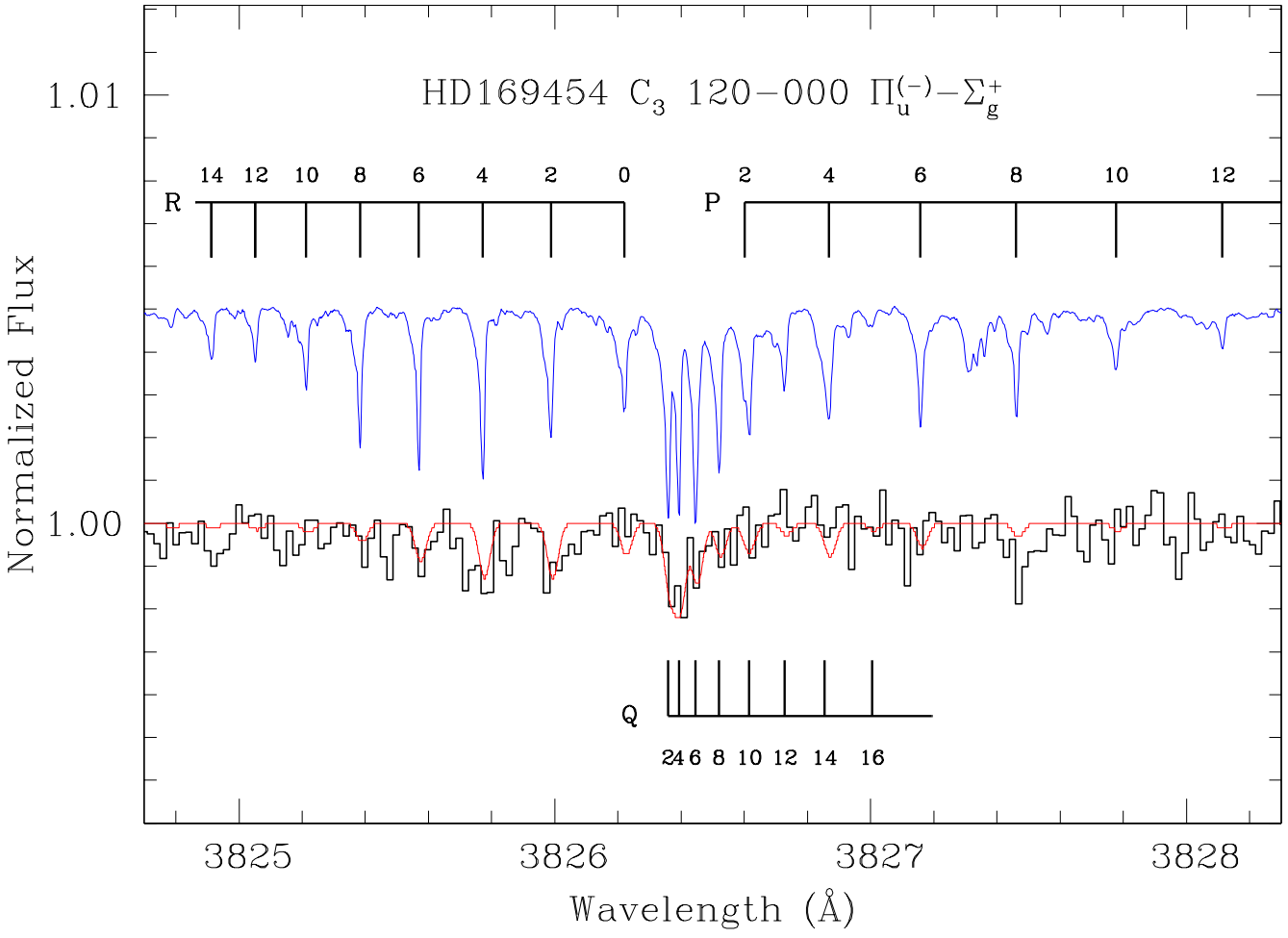

Positions of rotational lines are marked with thick lines.

Information on column densities in HD 169454

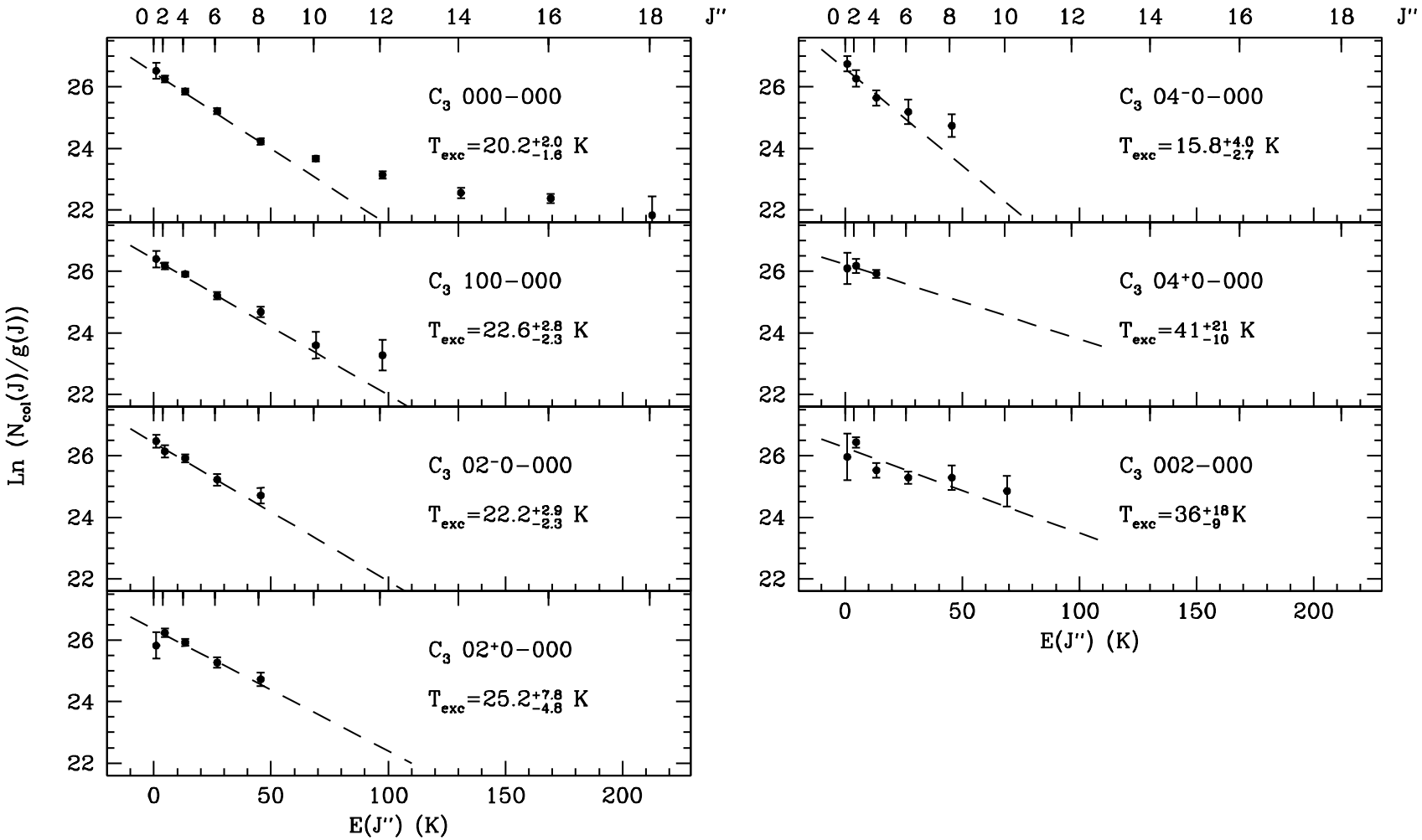

Column density distribution of C_3 $X^1\Sigma_g^+$ 000 rotational levels

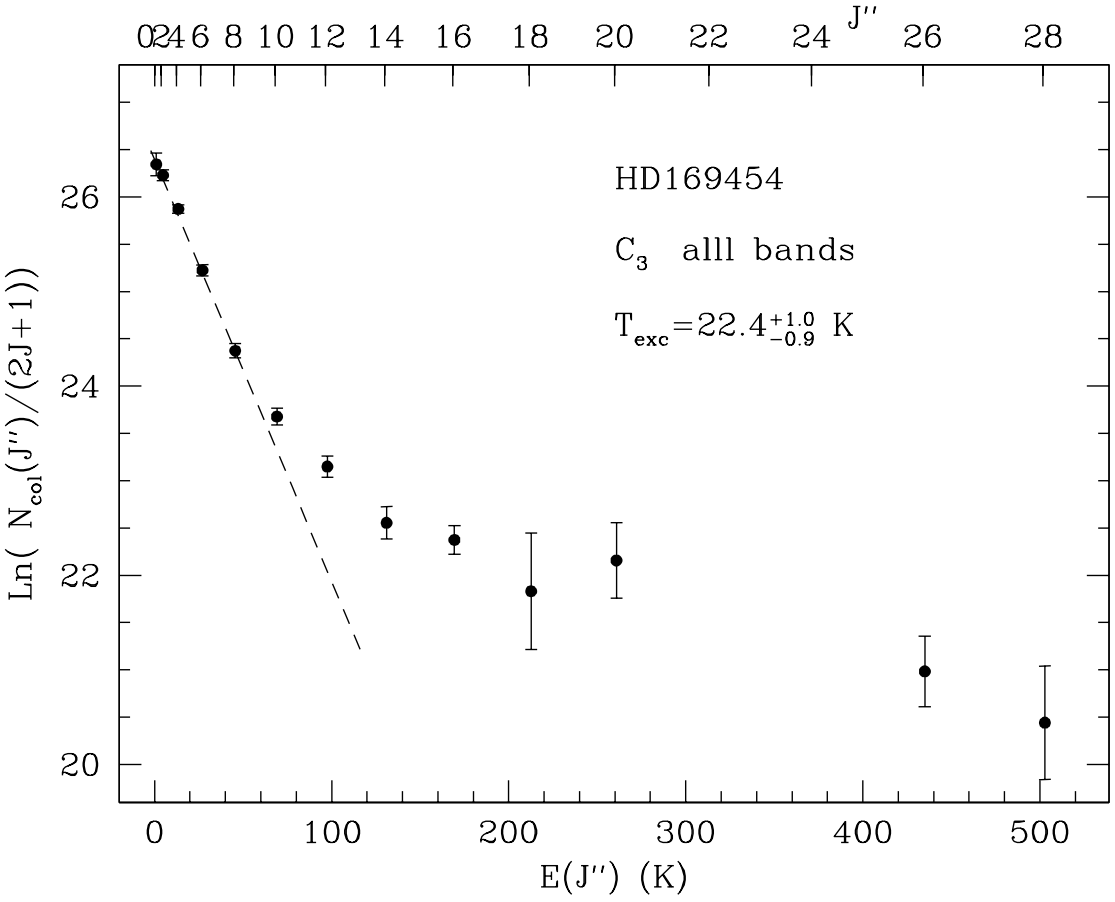

The dashed line shows the thermal population at 22.4 K obtained from the weighted linear fit to levels $J = 0, 2, 4, 6$.

The observed molecular column densities towards HD 169454.

Molecule	N_{col} (10^{12} cm^{-2})	T_{exc} (K)	Source
C_2	65±1	19±2	Kazmierczak et al. (2010)
	73±14	15^{+10}_{-5}	Jannuzi et al. (1988)
	70±14		Oke et al. (2002)
	160±29		Adamkovics et al. (2003)
C_3	6.61±0.19	22.4±1.0	Schmidt et al. (2014)
	2.24±0.66	23.4±1.4	Adamkovics et al. (2003)
	4.5±0.3	42	Oke et al. (2002)
C_4	<4-40	∼120	this work
CH	39.6±0.3		Schmidt et al. (2014)
	46±8		Jannuzi et al. (1988)
	$36.5^{+12.6}_{-7.8}$		Crawford (1997)
CH^+	20.8±0.2		Schmidt et al. (2014)
H_2	(8×10^{20})		Schmidt et al. (2014)

The observed molecular column densities towards HD 169454.

Molecule	N_{col} (10^{12} cm^{-2})	T_{exc} (K)	Source
C_2	65±1	19±2	Kazmierczak et al. (2010)
	73±14	15^{+10}_{-5}	Jannuzi et al. (1988)
	70±14		Oke et al. (2002)
	160±29		Adamkovics et al. (2003)
C_3	6.61±0.19	22.4±1.0	Schmidt et al. (2014)
	2.24±0.66	23.4±1.4	Adamkovics et al. (2003)
	4.5±0.3	42	Oke et al. (2002)
C_4	<4-40	∼120	this work
CH	39.6±0.3		Schmidt et al. (2014)
	46±8		Jannuzi et al. (1988)
	$36.5^{+12.6}_{-7.8}$		Crawford (1997)
CH^+	20.8±0.2		Schmidt et al. (2014)
H_2	(8×10^{20})		Schmidt et al. (2014)

Excitation mechanism

Roueff et al. (2002) presented an excitation model of C_3 towards HD 210121. An interesting aspect of their approach was the inclusion of **destruction and formation processes** of C_3, in view of its short life time in typical diffuse clouds.
As a consequence, **the initial population of the highest rotational levels in the formation process may not change** significantly by collisions before the molecule is destroyed by photodissociation.
The excitation model provide us information on the local gas density and gas temperature (C_2).

Excitation mechanism - assumptions

- when C_3 is formed with initial population of levels is well described by the formation temperature, T_f of order of 150-300 K
- C_3 is destroyed by the photodissociation process, D$\sim$0.5 10^{-9} s^{-1}
- in C_3 dipole rotational transitions are forbidden, quadrupole transitions left
- levels are excited by collisions with H_2 and He
- and through far infrared pumping

C3 excitation model - results

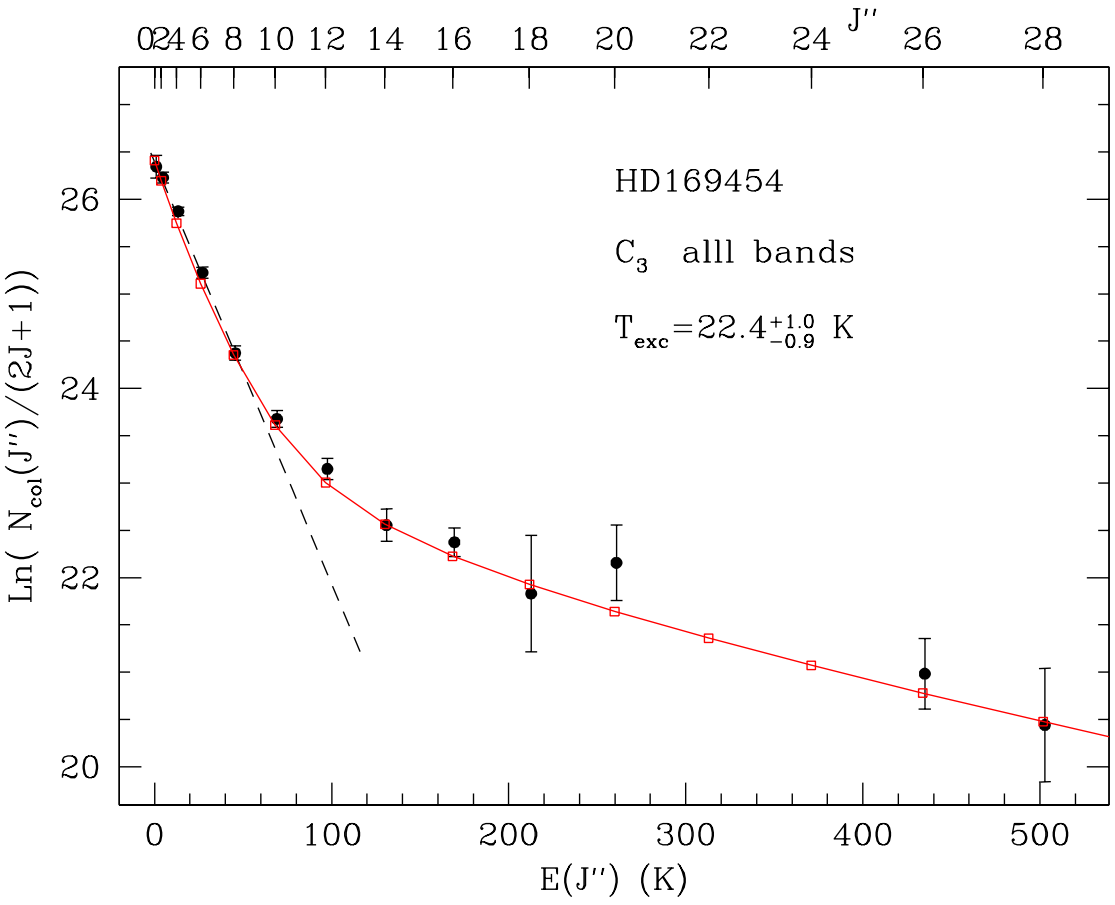

The solid red line show the predictions of the excitation models of Roueff et al. (2002) for n_{H_2}=1000 cm^{-3}, T_{gas}=16 K, D=1$\times$10^{-9} s^{-1}.

C3 excitation model

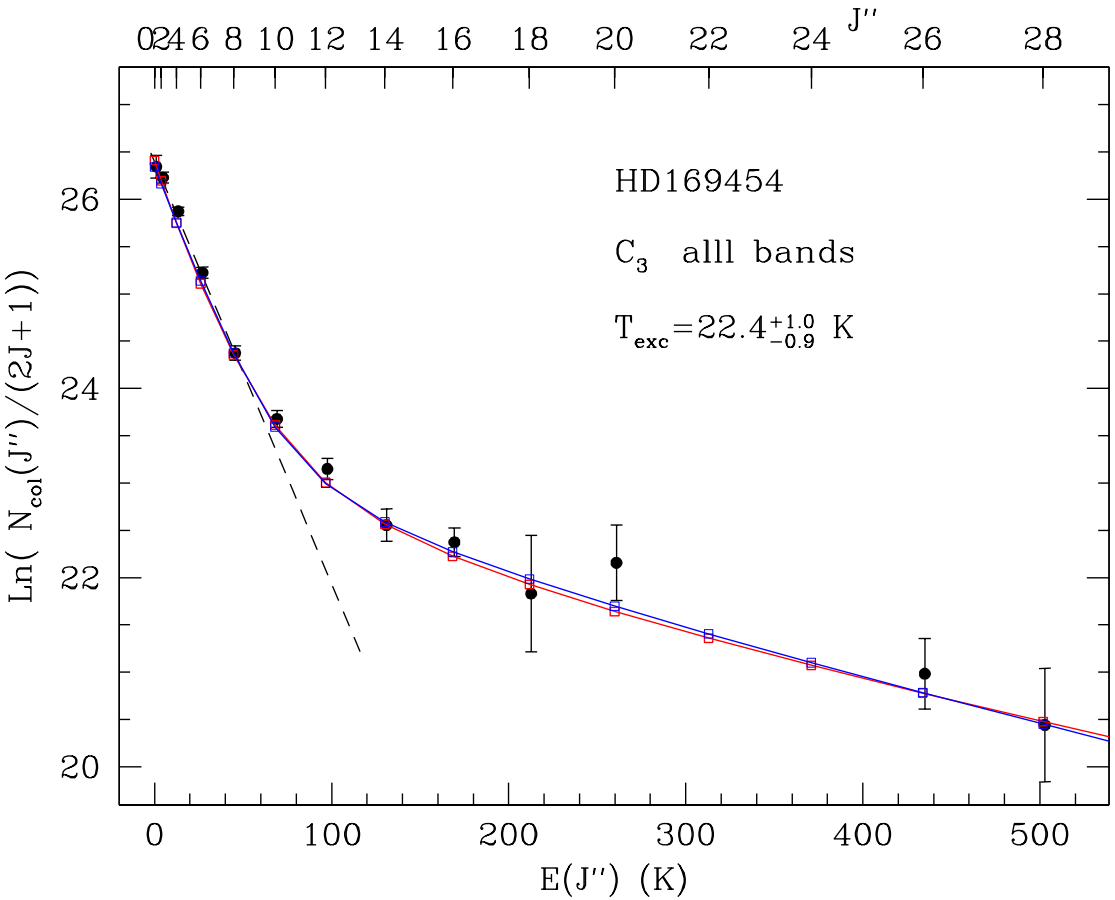

The solid blue line show the predictions of the excitation models for n_{H_2}=500 cm^{-3}, T_{gas}=18 K, D=12$\times$10^{-9} s^{-1} and collisional rates of Ben Abdallah et al. (2008).

Excitation mechanism - conclusions I.

- a one parameter family of models may be constructed as a function of the gas density, here assumed to be composed of molecular hydrogen, the density n_{H_2} is varied in a range between 400 and 5000 cm^{-3}
- the best fits for fixed densities n_{H_2} are described by the following sets of (n_{H_2}, T_k, D) parameters: (400 cm^{-3}, 12 K, 0.5×10^{-9} s^{-1}), (500 cm^{-3}, 13 K, 0.6×10^{-9} s^{-1}), (1000 cm^{-3}, 16 K, 1×10^{-9} s^{-1}), and (5000 cm^{-3}, 18 K, 5×10^{-9} s^{-1})
- the formation temperature T_f is determined at 300^{+50}_{-30} K.
- for higher densities above $n_{H_2} = 1000$ cm^{-3}, one observes that the population distribution depends on the ratio of the collisional rate to the destruction rate, $n_{H_2} q_{ul}/D$, with q_{ul} the rate coefficient

Excitation mechanism - conclusions II.

- when new collisional rates of C_3 - He of Ben Abdallah et al. (2008) are used then:
- the parameters of the best fit models are changed
- the two exemplary models characterized by set of (n_{H_2}, T_k, D) parameters: (500 cm^{-3}, 18 K, 12×10^{-9} s^{-1}) and (1000 cm^{-3}, 18 K, 24×10^{-9} s^{-1}), the uncertainty of the formation temperature in this approach is estimated at $T_f = 250^{+50}_{-30}$ K.
- the best fit dissociation rates much above accepted values $.5 \times 10^{-9}$ s^{-1} (van Dishoeck 1988).

Excitation mechanism - final conclusions

- the excitation model parameters sensitive to collisional rates
- much to high parameter of the photodissociation rate, found 10^{-8} s^{-1}, expected $0.5\,10^{-9}$ s^{-1} when new collisional rates are used

C_2 and C_3 formation in diffuse clouds

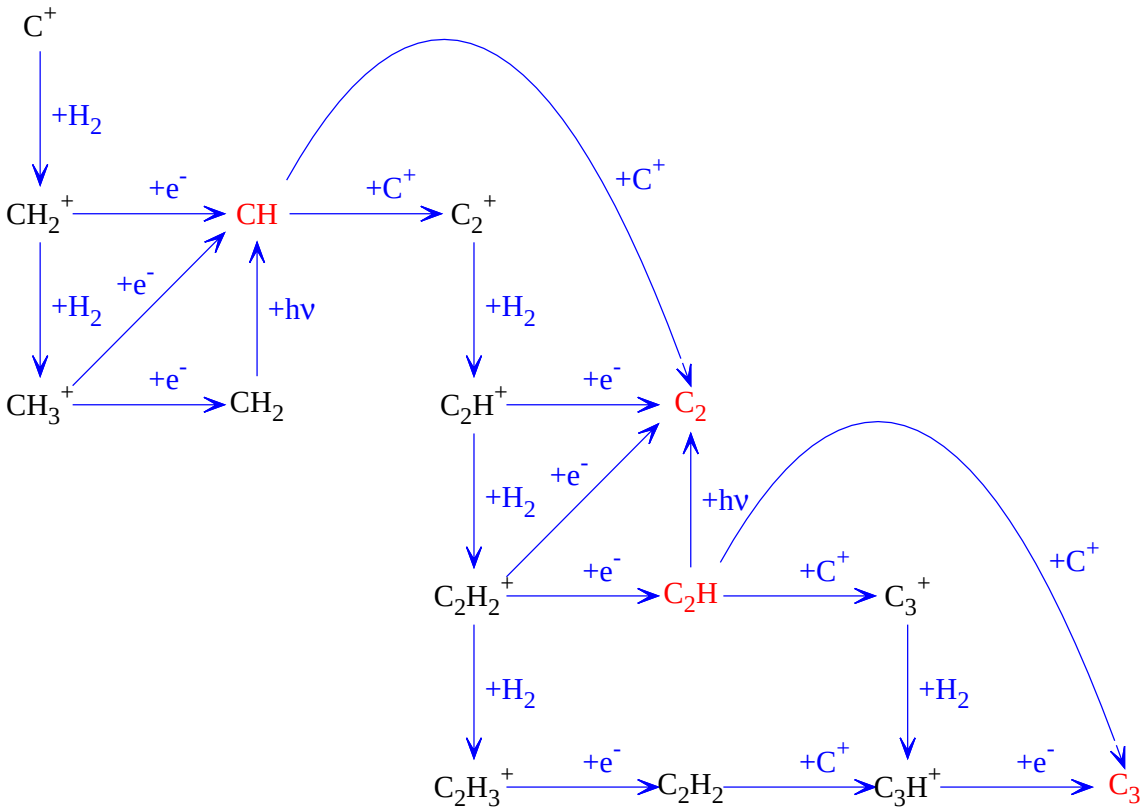

Schematic outline of chemical reactions connected with C_2 and C_3 formation.

C_2 and C_3 formation in diffuse clouds

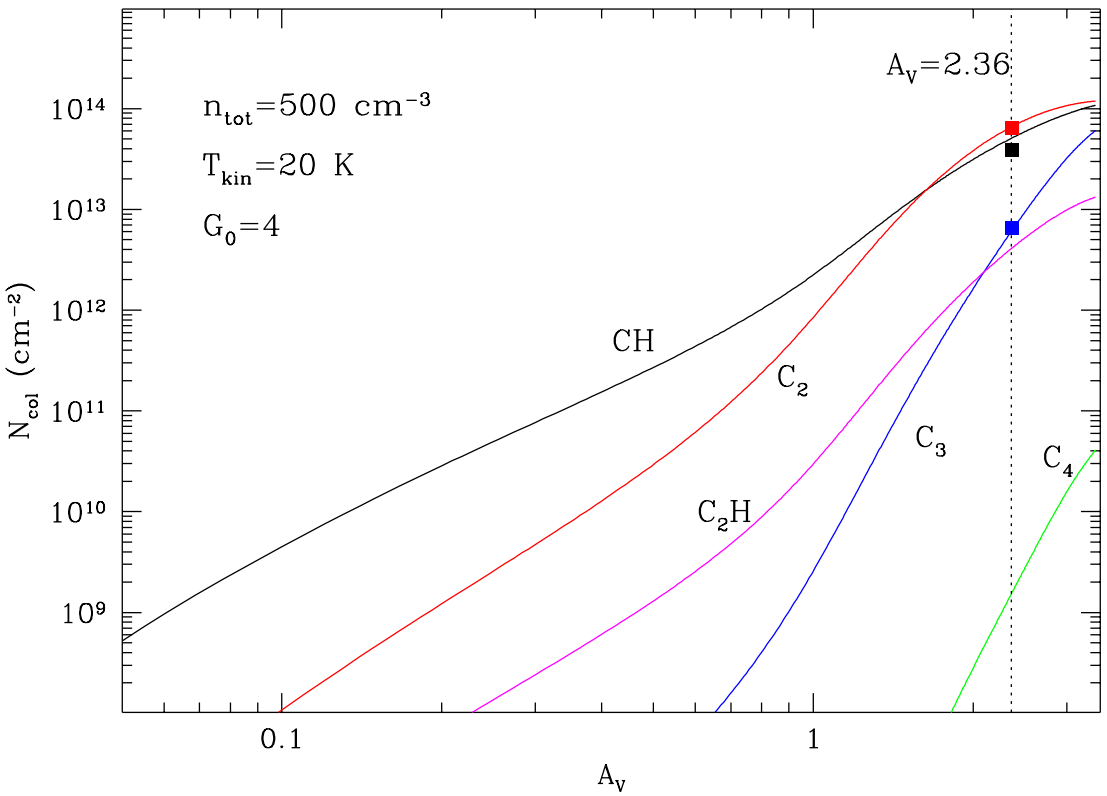

Abundances of CH, C_2, C_3, and C_4 carbon species computed as a function of the total visual absorption A_V (PDR-Meudon code). C_2H toward HD169454 - with IRAM - expected T_{mb} few to tens mK.

Summary

- for the first time 8 vibronic bands of the cometary system are identified in diffuse cloud
- high level of spectral details including pertubed states
- the observed transitions constrain excitation model